SACLANTCEN REPORT
serial no: SR-302

SACLANT UNDERSEA RESEARCH CENTRE REPORT

GENERIC OCEANOGRAPHIC ARRAY TECHNOLOGIES (GOATS)'98 – BI-STATIC SEABED SCATTERING MEASUREMENTS USING AUTONOMOUS UNDERWATER VEHICLES

H. Schmidt, A. Maguer, E. Bovio, W.L.J. Fox, K. LePage, N.G. Pace, P. Guerrini, P.A. Sletner, E. Michelozzi, B. Moran, R. Grieve

October 1998

The SACLANT Undersea Research Centre provides the Supreme Allied Commander Atlantic (SACLANT) with scientific and technical assistance under the terms of its NATO charter, which entered into force on 1 February 1963. Without prejudice to this main task – and under the policy direction of SACLANT – the Centre also renders scientific and technical assistance to the individual NATO nations.

Generic Oceanographic Array Technologies (GOATS)'98 – Bistatic Seabed Scattering Measurements using Autonomous Underwater Vehicles

H. Schmidt, A. Maguer, E. Bovio,
W.L.J. Fox, K. LePage, N.G. Pace,
R. Hollett, P. Guerrini, P.A. Sletner,
E. Michelozzi, B. Moran, R. Grieve

The content of this document pertains to work performed under Thrust 03 of the SACLANTCEN Programme of Work. The document has been approved for release by The Director, SACLANTCEN.

Jan L. Spoelstra
Director

intentionally blank page

Generic Oceanographic Array Technologies (GOATS)'98 – Bistatic Seabed Scattering Measurements using Autonomous Underwater Vehicles

H. Schmidt, A. Maguer, E. Bovio,
W.L.J. Fox, K. LePage, N.G. Pace,
R. Hollett, P. Guerrini, P.A. Sletner,
E. Michelozzi, B. Moran, R. Grieve

Executive Summary:

Unmanned underwater vehicles (UUV) are important assets in many aspects of naval operations, most notably shallow and very shallow, littoral MCM scenarios. Following the development of rapid, compact computer technology and advanced control concepts, autonomous underwater vehicle (AUV) technology has become an attractive alternative to otherwise tethered remotely operated vehicles (ROV) in the operational context.

Because of the space and power requirements of sensors such as bottom imaging or mine hunting sonars, naval AUV development has initially been centred around relatively large vehicles. The price of such vehicles restricted this new technology to very special operations where cost was a minor issue.

The new autonomous ocean sampling network (AOSN) concept has the potential of making this technology available to a much wider scientific and operational community. The AOSN concept, developed by a partnership of US academic institutions and Navy laboratories, supported by the Office of Naval Research, combines small and inexpensive AUV's with state-of-the-art communication technology, to create a network of mobile sensor platforms, which may be operated independently or together to optimally measure properties of the ocean environment.

The GOATS'98 experiment addressed some of the fundamental scientific and systems issues associated with adapting this new multi-platform concept to MCM operations in shallow and very shallow littoral environments, including rapid environmental assessment (REA) and MCM sonar.

Specifically, the experiment provided a unique data set of three dimensional target scattering and reverberation in shallow and very shallow water. These data will be important both for model validation and for identification of features of the 3-D acoustic field which distinguish targets from reverberation and can be measured by an AUV network.

Systems oriented objectives of the experiment were associated with the oper-

ation of an AUV from an offshore platform, including navigation and control in shallow and very shallow water, launch and recovery procedures and the feasibility of using state-of-the-art AUV technology as high-fidelity acoustic platforms.

The GOATS'98 experiment clearly demonstrated that small and inexpensive AUV's can be operated reliably in shallow and very shallow water, launched and recovered from an offshore surface ship. It was also demonstrated that AUV technology is an excellent acoustic platform for new sonar concepts for littoral MCM.

Generic Oceanographic Array Technologies (GOATS)'98 – Bistatic Seabed Scattering Measurements using Autonomous Underwater Vehicles

H. Schmidt, A. Maguer, E. Bovio,
W.L.J. Fox, K. LePage, N.G. Pace,
R. Hollett, P. Guerrini, P.A. Sletner,
E. Michelozzi, B. Moran, R. Grieve

Abstract:

The GOATS'98 experiment was performed May 5-29, 1998 in shallow water off Marciana Marina, on the island of Elba, Italy. The experiment addressed some of the fundamental issues associated with using the new Autonomous Ocean Sampling Network (AOSN) concept for mine countermeasures and rapid environmental assessment in shallow, and potentially very shallow water. A parametric source mounted on a tower was used to insonify proud and buried seabed targets. Target scattering and reverberation were measured by several fixed arrays and a mobile array mounted on an autonomous underwater vehicle. This extensive receiving array capability was used to map the full 3-D structure of scattering and reverberation, the objective being to identify 3-D acoustic features which distinguish targets from the reverberant background and which may, therefore, be exploited for combined detection and classification. The concurrent use of the AUV addressed various issues associated with the use of the AOSN concept for measuring such features by providing mobile platforms for both mono, bi and multistatic sonar configurations. The experiment demonstrated clearly that AUV technology is now sufficiently mature to enable small, inexpensive vehicles to be operated reliably in very shallow water, launched and recovered from a surface ship offshore. The excellent quality of the 3-D acoustic data sets recorded during the experiment demonstrated that AOSN technology should provide extremely useful acoustic platforms for new sonar concepts in littoral MCM.

Keywords: mine countermeasures ∘ sonars ∘ reverberation ∘ target scattering ∘ shallow water ∘ underwater vehicles

Contents

1

Introduction

Unmanned underwater vehicle (UUV) technology has made significant progress during the last decade. Remotely operated vehicles (ROV) are standard equipment in ocean science, the offshore industry, and most navies. From an operational point of view it is desirable to perform a transition from ROV to autonomous underwater vehicle (AUV) technology, eliminating the need for a tether connecting the vehicle with a surface ship or a submarine. Today's AUV's are capable of reaching more than 90% of the ocean volume with a wide spectrum of applications, e.g., acoustic imaging of abyssal plains, maintaining offshore installations, or scientific measurements in hitherto inaccessible parts of the ocean. However, because of the space and power requirements of sensors such as bottom imaging or mine hunting sonars, AUV development work has initially been centred around relatively large vehicles. The price of such vehicles restricted this new technology to very special operations where cost was a minor issue. Therefore, these vehicles have never reached the general academic, industrial or naval communities as a general-purpose platform.

The new autonomous ocean sampling network (AOSN) concept [1] has the potential of making this technology available to a much wider scientific and operational community, with significantly enhanced access to all parts of the world's oceans as a result. The AOSN paradigm, developed by a partnership of US academic institutions and Navy laboratories, supported by the Office of Naval Research, combines small and inexpensive AUV's with state-of-the-art communication technology, to create a network of mobile platforms, which may be operated independently or together, to optimally measure properties of the ocean environment.

The feasibility of the AOSN concept, as an integral component of ocean observation and prediction systems, has already been demonstrated for a coastal environment with strong frontal structures (Haro Strait'96) [2], and for a deep ocean environment with abundant convective circulation (Labrador Sea'98) [3]. In both cases, the AOSN added a measurement component to a more general scientific experiment which could not have been achieved in any other way. This 'science-driven' technology development has been a key feature of the entire AOSN effort, which is continuing through several multi-disciplinary science and technology efforts in the US.

While most of the AOSN effort has so far been focusing on environmental assessment, there are several other application areas within the navy context. However, for these

applications to take advantage of this emerging technology, it is in general necessary to rethink the operational procedures. For example, the small AOSN platforms are inadequate for carrying many of the sonar systems currently used from typical navy platforms, with the exception of those carried by divers. Therefore, to maintain adequate system performance, it will in general be necessary to not only redesign the sensor suites, but also the entire mode of operation. For example, the AOSN is ideally suited for bi- and multi-static sonar concepts with sources and receivers on different platforms, an option which in the past has received little attention because of the reliance on single, large platforms.

The GOATS'98 experiment was aimed at exploring some of the fundamental aspects of adapting the AOSN technology to mine countermeasures in shallow and very shallow water. It was planned and executed in a partnership between SACLANTCEN, Massachusetts Institute of Technology (MIT) and the US Office of Naval Research (ONR). The experiment was aimed specifically at developing an improved fundamental understanding of the physics of three dimensional acoustic scattering from proud and buried objects and the associated seabed reverberation in shallow, littoral environments. The long-term objective of this effort is to develop new sonar concepts and systems which exploit the significant information about target characteristics available in the 3-D multistatic field, and to achieve improved detection and classification performance for buried targets in particular.

The GOATS'98 experiment provided a first step towards the development of such future MCM sonar concepts, by achieving a unique measurement of full three dimensional scattering by man-made and natural objects along with the associated seabed reverberation, while at the same time demonstrating the use of small AUV's as acoustic receiver platforms for MCM and their potential for rapid environmental assessment, in shallow littoral environments.

The data acquired during the experiment will validate new seismo-acoustic bottom-interaction models, such as the MIT OASES-3D [4] and the Helmholtz-Kirchoff model [5] developed at SACLANTCEN, both of which have been applied successfully to model the penetration observed in the SACLANTCEN MCG1-97 experiment [6]. This analysis has lead to a new fundamental understanding of the controlling physical mechanisms of direct evanescent coupling and seabed scattering, depending on the frequency regime.

Building on the methodology and results of the MCG1-97 and MCG2-97 experiments, GOATS'98 focused on the fundamental issues regarding detection and classification of buried targets, using physical and synthetic 3-D arrays. The detection and classification potential of multistatic configurations will be explored by investigating the differences in the 3-D characteristics of seabed reverberation and target returns. Since both aspect-dependent targets and seabed ripples produce strongly anisotropic scattered fields, the differences in their spatial and temporal structure may be better

exploited by multistatic sonar configurations, with potential for both detection and classification performance enhancement compared to the more classical monostatic systems [7].

With the limited spatial coherence of target signals, the new multistatic sonar concepts will exploit the differences in scattering directionality between targets and reverberation. It will therefore be crucial to accurately predict the reverberant field. At sub-critical angles in particular, the seabed roughness is expected to be the dominant reverberation mechanism, and for anisotropic ripple features in particular, the reverberation becomes strongly aspect dependent [7]. The measurement of seabed roughness is therefore critical. One of the advantages of the new AUV technology is sensor flexibility, and there are various candidate multi-beam and sidescan sonar systems applicable to assessment of bottom roughness. Such seabed imaging systems will be applied in future experiments, but in GOATS'98, a very simple concept was investigated, using an echosounder source on an AUV in conjunction with the vehicle's acoustic array. Using conventional and synthetic aperture processing, the echosounder reverberation will be inverted for seabed roughness characteristics using scattering models. If successful, this concept can be applied for 'through-the-sonar' rapid environmental assessment.

2

Issues and objectives

The overall, **long-term objective** of the GOATS effort is to address in a coordinated fashion the scientific and technological issues associated with the development of a new MCM sonar concept for shallow water and littoral MCM operations, based on a synergy of new, inexpensive or expendable, autonomous platform and sensor technologies and a new class of processing approaches which take optimal advantage of scattering and propagation physics in shallow waveguides and the more flexible measurement capabilities of the platforms.

The specific objectives of GOATS'98 are of a fundamental physics, modeling, and systems nature. The *physics* issues addressed are:

- Determine the spatial structure of the **scattering** from axisymmetric and **aspect-dependent targets**. The anisotropic spatial structure of the target field is critical to detection and classification enhancement of bi and multistatic MCM concepts. Modeling suggests that higher signal-to-reverberation ratio may be achieved in multi-static configurations [7].
- Explore the spatial structure and statistics of **multistatic reverberation** from the sonar beam footprint produced by isotropic small-scale roughness, sediment inhomogeneities, and anisotropic seabed features such as sand ripples. The performance enhancement of multistatic systems depends highly on exploring differences in the spatial structure of the target and reverberant fields, both for proud and buried targets. GOATS'98 is expected to provide an experimental validation of this concept.
- The **frequency dependence** of mono- and bistatic target scattering and reverberation is of significant consequence to the detection and classification of buried objects. Modeling studies [7] and analysis of MCG2-97 data [9] strongly suggest that significant gains can be achieved by operating at lower frequencies (1-3 kHz). In this regime, the evanescent penetration coupling is strong and at the same time reverberation from rippled seabed, depending on the low-wavenumber roughness components, may drop off below 5 kHz [7]. This hypothesis will be validated by GOATS'98 through extensive 3-D sampling of the scattered fields.
- **Waveguide effects.** The shallow water waveguide has a significant multipath

structure, which is a severe limitation for classical systems and processing approaches. New multistatic systems, with fixed or synthetic arrays, may be able to explore the information carried in the multipath structure, provided the structure produced by targets has significantly different spatial statistics to those of reverberation. For example, various models show that a buried target will radiate predominantly in a cone confined by the critical angle, while the return at sub-critical angles will be associated with the weaker evanescent coupling ('tunneling') effect [7]. Therefore, the first multiples may provide a signal with significantly better signal-to-reverberation ratio than the direct target return, both in monostatic and multistatic configurations. This hypothesis is supported by both the model predictions and preliminary analysis of the data collected during MCG2-97 [9]. If verified and provided the effect is robust in regard to the environmental conditions, this effect may be a key to expanding the coverage of MCM detection systems.

Efficient wave-theory models are currently being developed for 3-D scattering and propagation in stratified, shallow water waveguides [4, 7]. The efficiency of these models is achieved by applying approximations to the handling of the scattering process and its coupling back into the waveguide propagation. The central *modeling issue* of GOATS'98 is therefore

- **Validation** of the OASES-3D modeling capability for accurately representing the physics of bottom target scattering and reverberation. Key issues are the validity of perturbation theories for 3-D rough interface reverberation and the validity of the single-scattering approximation for buried targets.

The new AUV technology provides a number of opportunities for **rapid environmental assessment** using acoustic and non-acoustic sensors. A particularly critical environmental parameter for MCM is the seabed roughness characteristics. In terms of system cost, it would be desirable to perform 'through-the-sonar' REA. A possible solution is to use a simple low-frequency source, e.g., a standard 8 kHz echosounder, on an AUV already equipped with acoustic receivers and then use array processing techniques to invert for seabed properties. A demonstration of the feasibility of such a concept was one of the major environmental assessment objectives of GOATS'98.

The *MCM systems* oriented issues are associated with both the detection and classification issue and the use of new underwater vehicle technology for MCM applications.

- Evaluate the feasibility of detecting buried mines at *sub-critical* angles in mono- and multistatic configurations.
- Determine the potential of using long, physical aperture arrays, for improving **detection** of buried mines. Especially for working at lower frequencies where

the bottom penetration is better, a large aperture will increase the azimuthal resolution and should therefore improve the signal-to-reverberation ratio.

- Demonstration of new **AUV** technology for synthetic array platforms for multistatic MCM sonars as an alternative to physical acoustic arrays. Specific issues concern the effects of vehicle noise, autonomous handling of large dynamic ranges of received signals, small-scale platform navigation and control, acoustic communication in shallow water, and adaptive sampling strategies.
- Demonstrate the use of small AUV's for **rapid environmental assessment** for MCM operations in denied littoral areas. Issues include water column assessment and seabed characterization. Roughness characterization is particularly important with regard to discriminating targets from reverberation in the 3-D acoustic field.

3

Experimental approach

The GOATS'98 experiment was carried out 5-29 May, 1998 in 12-15 m deep water off the pier at Marciana Marina, the island of Elba, Italy. Prior to the experiment a number of spherical and cylindrical targets were buried at different depths, within a 10x10 m area of sandy bottom (Fig. 1). The test area, located approximately 100 m north of the pier access, was the site used for MCG2-97, with a 1000 m^2 (approx.) patch of sand surrounded by a rocky bottom. The thickness of the sand was several metres and provided excellent data for the penetration and target scattering study in MCG2-97.

The initial phase of the experiment was devoted to equipment deployment and environmental assessment of the test area, with the *Manning* using a boomer for sub-bottom characterization and EM-3000 multi-beam and 100 kHz side-scan systems for seabed characterization. Other site survey measurements included coring, with measurement of porosity, sound speed, density, and permeability. These parameters are important for assessing the frequency-dependence of the sound speed. The roughness of the target area was assessed using stereo-photography. Shear properties were inferred from small scale seismic experiments, with the buried hydrophone array acting as receivers and a shotgun-source as generator of Scholte waves.

The major component of GOATS'98 was the measurements of 3-D scattering by proud and buried targets, and the associated reverberation environment. For insonification of the seabed the same TOPAS rail facility used in MCG2-97 was applied [6]. It is well proven and robust, important considerations when many different resources are utilized. A combination of fixed and mobile arrays was applied for recording the 3-D scattering and reverberation from targets and seabed. One was a 16-element line array, mounted vertically in a monostatic configuration on the TOPAS trellis. Another was a 14-element buried hydrophone array. This array was also used for measuring seismic waves produced by a shotgun source, in order to characterize the sediment shear properties. The AUV was equipped with an 8-element line array in the nose, and a self-contained acquisition system. The Centre's new 128-element array was used to provide a fixed reference to the mono and bistatic measurements collected on the mobile AUV array.

The AUV operations were performed from the R/V *Alliance*, anchored approximately 600 m offshore. The AUV operations had two main components. The first

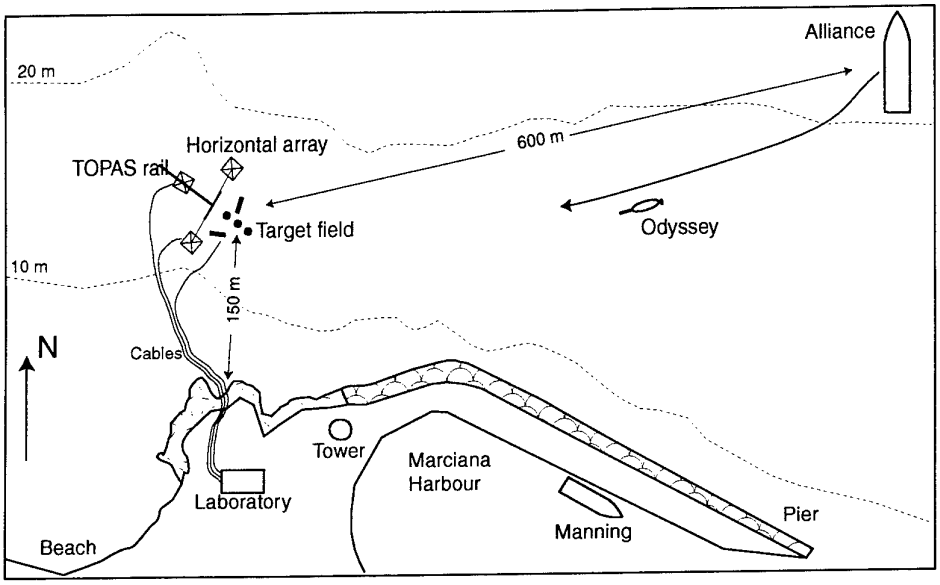

Figure 1 *Schematic (not to scale) of GOATS'98 operational scenario at Marciana Marina. T/B* Manning *deployed the TOPAS source facility and the fixed arrays near the target area. A shore laboratory controlled the TOPAS source and recorded data from a 16-element vertical array, a 128-element horizontal line array, and a buried hydrophone array. Alliance anchored offshore was used as a platform for the AUV operation and data processing centre.*

concerned the feasibility of using this technology for rapid environmental assessment (REA), specifically acoustic seabed characterization, in denied areas. For insonifying the seabed, the AUV was equipped with an 8-16 kHz echosounder source during the part of the experiment addressing this issue. During this REA phase, the AUV was launched from *Alliance* to perform survey missions in very shallow water close to the coastline, navigated by an acoustic long baseline (LBL) navigation system and an ultra short baseline (USBL) tracking system.

The primary mode of operation for the AUV was to perform a dense spatial sampling of the three dimensional scattered field, from the targets and the seabed reverberation, during TOPAS transmissions. In this mode the echosounder source was removed and the AUV was launched from *Alliance* to transit autonomously to the test area, where it performed various survey patterns over the targets, refined throughout the experiment to optimally collect both back- and forward scattering and reverberation.

4

Experimental resources

4.1 TOPAS rail facility

The TOPAS (TOpographic PArametric Sonar) [10] was used to insonify the targets and the seabed with a highly directional beam. The TOPAS transducer consists of 24 horizontal staves, electronically controlled to form a beam in a selected direction. It covers the frequency range 2-16 kHz for the secondary frequency and 35-45 kHz for the primary frequency. The transmitting source level is approximately 238 dB re 1 μPa @ 1m for the primary frequency. The source levels obtained at the difference frequencies vary from about 190 to 213 dB re 1 μPa @ 1m in the 2 to 16 kHz frequency band. A short single pulse is obtained by transmitting a weighted HF-burst at the primary frequency.

The broadband integrated source level obtained for different Ricker pulses of the low-frequency generated by the parametric sonar are given in Table 1.

Pulse	**Beam Width HF/LF (-3dB)**	**Band Width LF (-3dB)**	**LF SL (dB re 1 μPa @ 1m)**	**HF SL (dB re 1 μPa @ 1m)**
Ricker 8kHz	3° / 4°	6 kHz	201	238
Ricker 5kHz	3° / 4°	7 kHz	203.8	238
Ricker 4kHz	3° / 4°	6 kHz	202.6	238

Table 1 *Source level measurements*

A complete calibration of the TOPAS transmitter may be found in [11], while a description of the main functionalities of the TOPAS may be found in the operation manual from Simrad [10].

To allow insonification of the targets and the seabed at a wide range of incident angles, covering both the sub- and super-critical regimes, the transmitter was mounted on a tower fixed at 10 m above the seabed for this experiment. The tower in turn was mounted on a 24 m linear rail deployed on the bottom, along which its position could be precisely controlled using an electric motor, operated remotely from a shore laboratory. The TOPAS transmitter was mounted in a pan-and-tilt assembly with a motion reference unit (MRU) so that arbitrary transmission directions could be precisely controlled. Mechanical steering of the vertical angle, rather than elec-

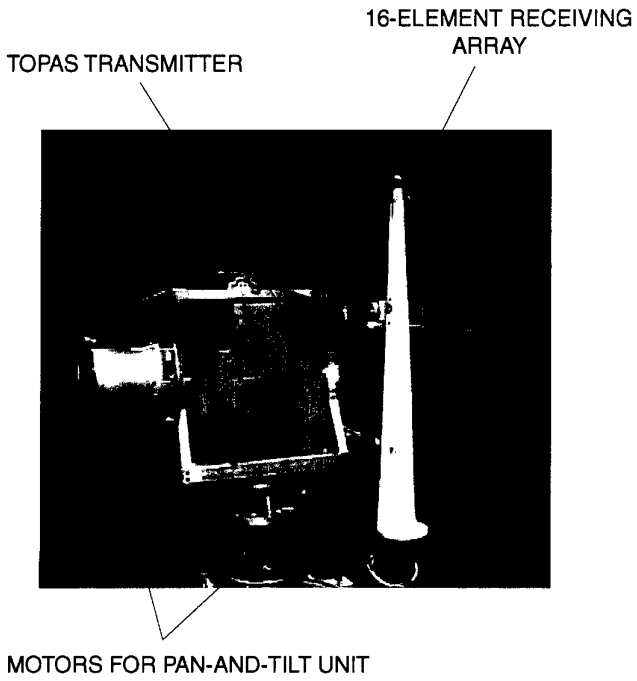

Figure 2 *TOPAS parametric sonar with pan-and-tilt unit and 16-element receiving array.*

tronic steering of the staves, was chosen to maintain a symmetric beam pattern [12]. Figure 2 shows the structure used to support the TOPAS parametric sonar. The vertically mounted 16-element array was used as one of the fixed receiving arrays.

Figure 3 shows the tower on which the sonar was mounted and the structure with four legs providing stability. This structure was mounted on a small trolley which travels along the rail. An underwater video camera was mounted on the structure to accurately measure the position of the tower on the rail.

The cables necessary to drive the transmitter, to lift and move the tower on the rail and for all the receiving arrays (16-element vertical array, 14-hydrophone buried array and 128-element horizontal array) were connected to a laboratory facility on shore. The layout of the target field and the location of the TOPAS rail and the receiving arrays are shown in Fig. 4.

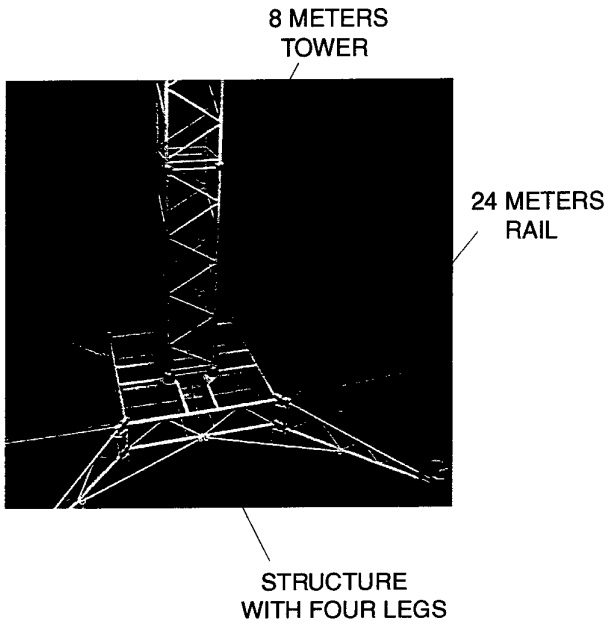

Figure 3 *TOPAS tower mounted on rail deployed on the bottom.*

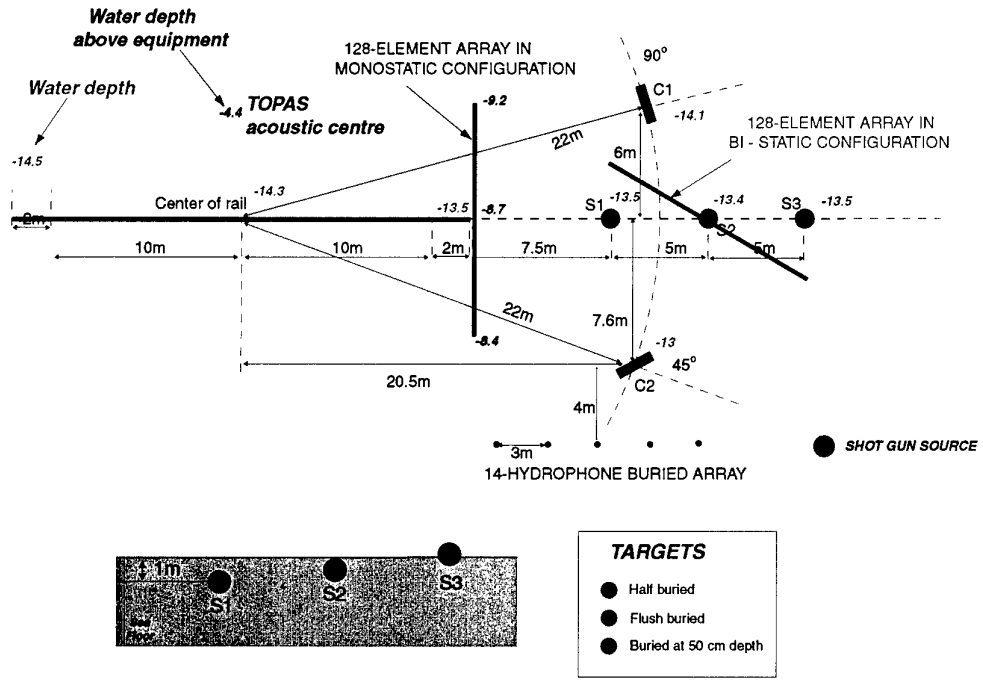

Figure 4 *Targets and arrays deployed in the test area.*

4.2 Targets

Five artificial targets were used in the experiment. Two of these were identical steel cylinders (C1 and C2), deployed with different orientations relative to the rail, as shown in Fig. 4. They were 2 m long and had a diameter of 50 cm. The thickness of the shell was 6 mm and both cylinders were filled with sea water. They were both flush buried in the sediment (i.e. just below the seabed). The main reason for having the different orientations for the cylinders was to emphasize the fundamental differences in the bistatic target returns, and also to be able to collect multiple aspect responses of a cylinder in relation to other work performed at SACLANTCEN on target classification.

Three identical spheres were deployed in line with the TOPAS rail at different burial depths(see Fig. 4). The spheres were identical steel shells of 1 m diameter and 3 cm wall thickness, and air filled. The sphere S3 was buried halfway into the sediment and the sphere S2 was flush buried in the seabed. The last one, S1, was buried at a depth of one radius (50 cm) into the sediment. The separation between the spheres was 5 m to allow them to be insonified independently by the TOPAS beam, and to reduce acoustic interference. The rationale behind having three identical spheres was to be

able to evaluate the variation of detection performance as a function of burial depth and grazing angle for both monostatic and bistatic configurations. Moreover, the dependency on burial depth of the spatial characteristics and resonance components of the backscattering can also be investigated .

The positions of the TOPAS tower on the rail used in this experiment and the corresponding incident grazing angles for all the targets are shown in Table 2. With a critical angle of approximately 24°, all targets were insonified at both sub- and super-critical incident angles.

Table 2 *Grazing angles on the five targets*

Rail position (m)	*Sph. S1*	*Sph. S2*	*Sph. S3*	*Cyl. C1*	*Cyl. C2*
0	18.7	16.2	14.7	17.6	17.6
5	22.7	18.7	16.2	20.5	20.5
7.5	24	20	17	21.9	21.9
10	27.1	22.2	18.7	24.4	24.4
12.5	30.5	24.4	20.3	26.4	26.4
15	34.6	27	22	29.9	29.9
17.5	39.8	30.5	24.4	33.4	33.4
20	46.5	34.6	27.1	37.4	37.4

4.3 Fixed acoustic arrays

Three fixed acoustic arrays of receiving hydrophones were used in the experiment. The first was a 16-element linear array designed to receive the secondary frequency band of the TOPAS transmissions (< 20 kHz), with element spacing of 9.4 cm. The array was mounted vertically in a near-monostatic geometry next to the TOPAS source, as shown in Fig. 2. The received signals were digitized and stored to disk by a workstation-based data acquisition system (DAS). These data were then available immediately over a small local network for quality checks and preliminary analysis.

The second fixed array consisted of 13 buried hydrophones and one hydrophone in the water column. The hydrophones were attached to five metal rods placed in a line, with a spacing of 3 m between the rods. Hydrophones were buried at depths of 10, 30, and 50 cm in the positions indicated in Fig. 4. This array was used to record signals generated by the seismic source (shotgun cartridge device). These data were recorded using the same DAS as the 16-element array.

The third fixed array was the new horizontal line array (HLA) which has 128 elements, spaced at 9.0 cm. The HLA was designed to be neutrally buoyant for towing, and to receive the secondary frequency band of the TOPAS. For this experiment,

the HLA was fixed in the water column, suspended 5 m above the seabed between two trellis towers. The array was deployed in two different configurations during the experiment, one measuring backscatter towards the source (approximately mono-static), and the other measuring bistatic scattering by being deployed above the targets (see Fig. 4). The signals from the array were appropriately conditioned and digitized onto a high-speed tape device. Spot checks of data quality were achieved by playing back selected runs and channels onto the workstation-based DAS.

With the extensive acoustic data collection capability, a total of 800+ Gbyte of acoustic data was collected at the shore laboratory during the experiment. Most of this (700 Gbyte) resulted from the 128-element array. It was the first time this array capability was used by the Centre and both the deployment and the data collection were successful. The data were of extremely high quality and will be important in regard to validating the computational models. This array was also used to record scattering of seismic energy generated by a small shotgun source deployed on the seabed.

4.4 Autonomous underwater vehicle

The *Odyssey II* class autonomous underwater vehicles were chosen as the mobile sensor platform for the GOATS'98 experiment because of their flexible architecture and proven performance. These vehicles have logged many hundreds of dives in 16 field deployments. The *Odyssey 'Xanthos'* used in GOATS'98 has logged close to 400 successful dives. A substantial fraction of the vehicle is dedicated to wet volume, which enables the *Odyssey II* vehicles to support a wide range of payload systems. Those fitted in the past include CTD, ADCP/DVL, ADV, side-scan sonar, USBL tracking systems, OBS, and several video systems. The core vehicle has a depth rating of 6,000 m, weighs 120 kg, and measures 2.2 m in length and 0.6 m in diameter. It cruises at approximately 1.5 m/s with endurance in the range of 3-12 hours, depending on the battery installed and the load. Included in the core vehicle are the guidance and navigation sensors necessary to support autonomous control: attitude and heading, pressure, altimeter, and LBL acoustic navigation.

4.4.1 Vehicle Configuration

The GOATS '98 experiment added two new payloads to the *Odyssey II* vehicle: an 8-element array mounted on the nose in a 'swordfish' configuration, and during parts of the experiment a rapid environmental assessment (REA) echosounder near the tail, (see Fig. 5). The former included an acquisition system, separately housed in the vehicle's wet volume, which required 100 W of power and generated data at a rate in excess of 5 Gbyte/hr. This system, the heart of the scientific payload for

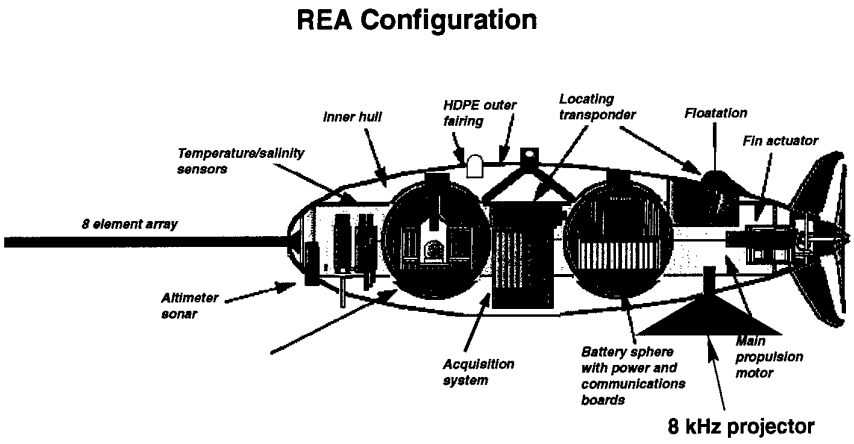

Figure 5 *Configuration of Odyssey II AUV 'Xanthos' for acoustic measurements in GOATS'98. The AUV control electronics and batteries are located in two 17" Benthos glass spheres. An 8-element array is mounted in a 'swordfish' configuration, and connected to a dedicated acquisition system in the centre well of the vehicle. The echosounder source was only applied for the REA missions, and removed during target scattering missions.*

the experiment, acquired signals from the TOPAS parametric source, the shotgun source, and the REA echosounder.

Further demands placed on the AUV by this experiment led to the inclusion of several sensors from within the *Odyssey* family of supported devices. These were a 200 kHz altimeter and an LBL acoustic navigation system. The altimeter enabled the AUV to survey at constant altitude (3-5 m) above the sea floor during the REA component of the field experiment and to avoid equipment placed on the bottom in the vicinity of the target field during the multistatic acoustics component. Figure 5 shows the *Odyssey II* class AUV *Xanthos* as configured for the GOATS '98 experiment.

Odyssey II AUV's contain a 3U VME main computer. It comprises a 40 MHz 68030 CPU with 8 Mbyte of RAM, an Ethernet controller, a SCSI controller and hard disk, and an 8-port serial card. The CPU card provides two additional serial ports, one of which acts as a dedicated console to the OS-9 real-time operating system. Attached to the multiple serial ports are the sensor and actuator subsystems. The actuators use the SAIL protocol, a multi-drop technique that uses addressing to allow multiple devices to share a single port.

4.4.2 Software

Odyssey vehicles are controlled using a behavior-based layered architecture. At the highest level, behaviors seek to achieve mission goals such as following a track line to a way-point. The layered controller generates high level commands which specify the desired speed, depth, and heading of the vehicle. Taking these commands as inputs, a PID dynamic controller generates the low-level commands which feed directly to the thruster and actuators. The layered control architecture allows the *Odyssey* to perform complicated adaptive missions such as bottom following surveys, or missions tracking isothermal contours, for example, while maintaining overriding safety procedures such as keeping a minimum distance from shore or avoiding obstacles.

4.4.3 Navigation

To allow the *Odyssey* to transect to the target area, accurately perform way-point navigation during its acoustic surveys, and avoid the fixed instrumentation such as the TOPAS tower and the HLA, a long baseline (LBL) acoustic navigation network was deployed at the beginning of the experiment. The LBL system comprised a 10-channel acoustic transceiver in the vehicle and a network of 4 transponders deployed around the survey area, with baselines of 200-300 m. The transceiver acoustically interrogates this net, typically at 9 kHz, and listens for the replies from each transponder. For the GOATS experiment the reply frequencies were 8.0, 8.5, 9.5, and 10.5 kHz. The multi-channel transceiver independently measures the time between interrogate and reply for all of the transponders. On-board navigation algorithms convert these times into slant ranges and calculate a position fix relative to the known transponder positions.

The performance of the LBL navigation system was improved throughout the experiment by first re-positioning the transponder network, and subsequently by iteratively re-tuning the network navigation using an error minimization procedure on the navigation data logged during two AUV missions. The resulting LBL navigation resolution was estimated to a few metres based on the navigation residuals. However, as discussed later, the micro-navigation using the acoustic signals and the altimeter detections of the HLA revealed a significant 5-10 m bias depending on the direction of the AUV.

4.4.4 Acoustic Array and Acquisition System

The acoustic array and acquisition system, developed at SACLANTCEN, consisted of a line array, mounted in the vehicle's nose, in a 'swordfish' configuration, and

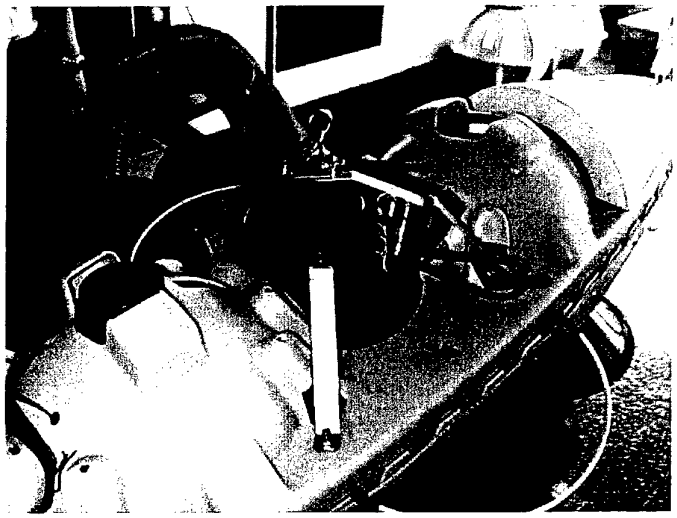

Figure 6 *AUV acoustic acquisition system mounted in centre well of Odyssey AUV.*

an autonomous data acquisition system, installed in a watertight canister in the vehicle's payload bay shown in Fig. 6.

The 'swordfish' array, shown in Fig. 7, is composed of kevlar strength members, plastic spacers and a 40 mm diameter polyurethane hose filled with oil, all suspended in a rectangular aluminum frame. The array is equipped with eight spherical hydrophones at 10 cm spacing. The array is connected to the acquisition system with a short underwater cable with 8 shielded twisted pairs.

The design of the acquisition chain for this experiment was not conventional for the following reasons:

- The sound source was a highly directional parametric transducer, requiring special signal conditioning to avoid saturation by the primary frequencies.
- The vehicle is autonomous, i.e. the gains can not be selected by an operator.
- The inter-modulation distortion of the electronic circuits must be much less than the difference of the source levels at the primary and the secondary frequencies of the parametric transducer
- The recovery time, after saturation by the direct sonar pulse, must be very short because the AUV is passing through the TOPAS beam during its surveys.

Each hydrophone signal was amplified with a variable gain differential stage and

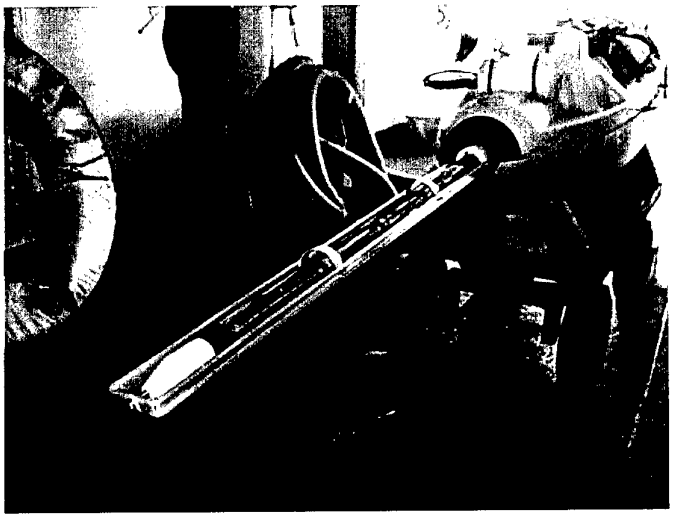

Figure 7 *8 element acoustic line array with 10 cm spacing, mounted on Odyssey AUV in 'swordfish' configuration..*

sent to two different circuits with selectable gains. The two output signals, after 'Bessel' type, switched-capacitor lowpass filters, were converted into digital form with 16 bit sigma-delta analog-to-digital converters (ADC). The entire acquisition chain was calibrated with two different settings of the low pass filters. The resulting system sensitivity curves are shown in Fig. 8.

The digital acquisition system, from the ADC's to the data storage disk, consisted of commercially available components, custom assembled and configured for the experiment. The system boards were housed in a VME card cage measuring 23 × 25 × 38 cm. The data storage disk was attached at the bottom of the cage. The cage provided room for a DC power supply,VME single-board CPU, and VME baseboard, sigma-delta ADC's and SCSI interface to disk. The single-board CPU provided a network connection to the *Alliance's* on-board computers, enabling download of the acquisition program prior to launch and retrieval of the acquired data at vehicle re-entry. The baseboard functioned as a base mounting and controller for the ADC and SCSI interface modules. The baseboard and modules were connected by a common internal bus, enabling high data transfer rates from the ADC module through the SCSI interface to disk. The ADC module provided a 16-bit conversion capacity of 16 channels at 100 kHz per channel sampling rate. The dynamic range available in the 16-bit conversion was further enhanced by acquiring the 8 channels of array data at two gain settings (preset prior to launch). The disk provided a storage capacity of 9 Gbyte, at sustained write speeds sufficient to store 16 channels at 50 ksample/s (1.6 Mb/s).

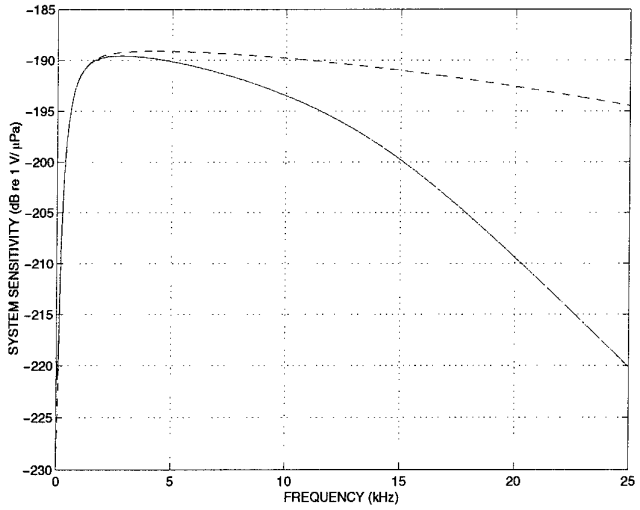

Figure 8 *The system sensitivity curves for the AUV acoustic acquisition chain (from hydrophones to ADC). The two curves represent the sensitivities for the two low pass filter settings: the solid curve for use with the TOPAS parametric source, and the dashed curve for use with the echo sounder*

Communication with the vehicle's control and navigation computer was performed via a serial port on the SCSI interface module. The synchronization of the data acquisition periods with the LBL navigation cycles and navigation data logging was achieved by notifying the vehicle's computer at the start of every 10-second acquisition cycle. The fusion of the acoustic data and the vehicle's log was achieved during the data retrieval phase by including the log in the headers of the data files at the moment of transfer to the on-board computers.

The system proved robust and capable of continuous operation in its sealed cannister, particularly during the long data retrieval periods on-board, without water cooling. The power consumption of the entire system was typically 100 W, supplied by the *Odyssey's* battery power supply via a 24 V line.

4.4.5 Echosounder projector

Bottom characterization is of paramount importance when dealing with buried targets [6]. The possibility of combining a MCM sonar capability with a REA component is one of the most important potentials of the multi-platform AOSN concept. For example, bistatic configurations are superior for assessing the geophysical properties of the sediment, because they directly measure the bottom reflectivity. Two

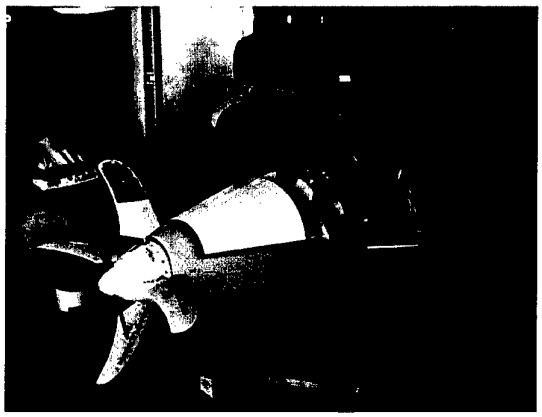

Figure 9 *Odyssey AUV mounted with 8-16 kHz echosounder projection for REA missions.*

or more AUV's within the network can perform such measurements and feed the information back to the network control vehicle, which can then adapt the sonar configuration to the environmental conditions.

Other environmental sensors can be housed on individual vehicles, as for example in this experiment, where a simple bistatic bottom characterization concept was investigated. An acoustic source was positioned at the rear end of the AUV, transmitting 8-cycle CW pulses alternately at 8 kHz and 16 kHz, at 60 ms intervals, with full beam widths of 50° and 25°, respectively. The source was calibrated at the two frequencies in terms of source levels and detailed beam patterns. Reception of seabed returns was via the 8-element 'swordfish' array in the nose of the AUV. The horizontal spacing between the source and the most distant receiver is 2.45 m, allowing bistatic measurements when the vehicle is within a few metres from the bottom. This is easily achieved with the *Odyssey* AUV which is capable of performing bottom-following surveys using altimeter readings to control pitch.

The source is a line-in-cone arrangement mounted outside the AUV fairing (see Fig. 9). There was some concern in advance as to the performance of the AUV with such a protuberance. During the data collection maneuvers the AUV did roll and pitch more than would have been expected without the cone, as described later, requiring significant motion compensation to be applied to the data. The 10 cm spacing of the receiving array allows the 8 kHz signals to be beamformed, which will be taken advantage of, in the detailed data processing.

4.5 Environmental assessment

4.5.1 Geophysical Survey

A geophysical survey of the test area was carried out, including sub-bottom profiling and coring. The sub-bottom survey was undertaken using a single array hydrophone on the sub-bottom profiler EG&G Mod.230. During the survey, the DGPS was not operational and the positions were determined with the ship's radar referred to a reference point on the jetty. Data was recorded on an EPC paper recorder and on a magnetic recorder (Sony PC 208A). Two cores were taken near the TOPAS rail, identified as Core no. 1 (40 cm), and Core No. 2 (33 cm). Core No. 3 (49 cm) was taken near the buried hydrophone array, on the TOPAS rail side.

4.5.2 Seafloor Survey

The seafloor mapping was performed using two different sensor systems:

- A high frequency swathe (300kHz) using a SIMRAD EM3000 multi-beam sonar system mounted on the bow of T/B *Manning*.
- A dual frequency (100kHz and 390kHz) sidescan sonar EG&G Mod.272 TD.

Both seafloor surveys were performed using DGPS navigation. The navigation of the sidescan survey was not compensated for the towing cable, because the half-buried target S3 provided a reference point, together with the rail and the TOPAS tower.

The sidescan sonar survey was performed at 100kHz to obtain information on the bottom morphology and at 390kHz to highlight the target area and the TOPAS rail. Data were registered on an EPC paper recorder and a magnetic recorder Sony PC 208A.

For assessing bottom roughness, a fully digital close-range stereo photogrammetry system was utilized [13]. In this process, two spatially separated cameras, mounted in a rigid frame, take digital photographs of a patch of the seabed. A height field is then produced via a stereo-correlation procedure. The system as configured for this trial, produced a height field over a 650 mm x 450 mm patch with effective resolution of roughly 1 mm in the horizontal and 2 mm in the vertical.

A waverider buoy was deployed in the experimental area to measure wave height. The buoy transmitted data to the shore lab where it was automatically stored by a small computer. Data were collected continuously from 16 May until the end of the experiment.

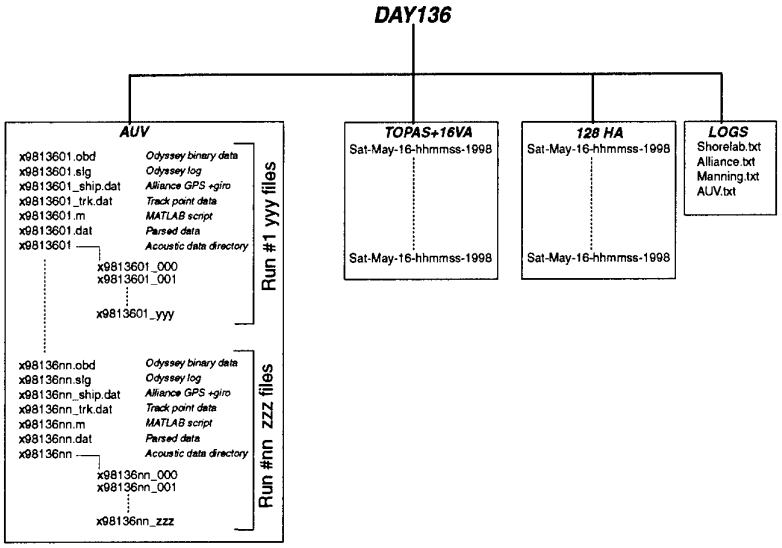

Figure 10 *Data infrastructure for day 136 (Saturday 16th May 1998)*

4.6 Data infrastructure

The experiment control and data processing centre was established on *Alliance*, although additional data processing was performed in the shore laboratory. The AUV data and those from the shore facility were catalogued on *Alliance*, together with all experiment logs. In order to synchronize the efforts in the shore laboratory and on *Alliance*, and for limited data transfer, a wireless local area network, based on Cylink spread spectrum radios, was established between the ship and the shore lab. In addition, the shore lab was connected to the Internet via a dedicated ISDN line to SACLANTCEN. This setup provided a 64 kbps Internet capability for both the shore laboratory and *Alliance*, and a 128 kbps connection between the two. The Internet connection was also used to demonstrate the transmission of video and audio from *Alliance* to SACLANTCEN.

A Web page for the experiment was established, with sub-pages in each of the laboratories. Part of the Web pages were open to public access, others were used exclusively for transfer of raw and processed data between the shore laboratory and the *Alliance*.

Figure 10 shows the organization of the data structure. The acoustic signals received on the 8 element array of the AUV were stored together with all relevant information recorded during each mission , and named according to the AUV lab convention:

x + Julian day + sequential run number for the day + specifier + extension

and where *specifier* can have the following values:

-ship for files with *Alliance* GPS and navigation information
-trk for files with Trackpoint data
-nnn for acoustic data acquired during cycle n (n=0,1,...,Nmax),

and where *extension* can have the following values:

obd for files with raw *Odyssey* replica binary data
m for Matlab script used to parse the *Odyssey* binary data
dat for parsed *Odyssey* binary data
slg for *Odyssey* log

The time of this data set is local time (=GMT +2 hours).

The acoustic signals received on the 16 element vertical array mounted on the TOPAS tower, were stored according to the ADAM format:

Weekday-Month-date-hhmmss-year

All relevant information related to the TOPAS transmission and to the parameters of the receiving chain is recorded in the header of each ping. The time of this data set is GMT.

The acoustic signals received on the 128 element horizontal array suspended above the target field were recorded on a high speed Datatape recorder as a continuous stream for the duration of each run. It was planned during the cruise to replay the tape after each run and to store in ADAM format the signals of the 128 hydrophones gated around the targets, but due to hardware problems in the acquisition/playback system, this was not possible. In order to verify the quality of the data, a few runs were replayed sending 32 hydrophones (1 every 4) to the analog output of the ICS system and acquiring them with the ADAM system. As soon as the hardware problem is resolved, all runs will be replayed as planned and stored in ADAM format.

All narrative information logged during the experiment was collected and consolidated into a single directory for each day. All data were backed up on tape cartridges and optical disks.

5

Examples of preliminary experimental results

Close to a Tbyte (10^{12} bytes) of data was collected during the environmental assessment and acoustic measurement portions of the experiment. The following section presents an overview of the types and the quality of the scientific data collected. In addition, examples of the preliminary processing work are given, most of which was performed during the actual cruise. This 'real-time' data processing was crucial to the success of the experiment, which was dependent on a multitude of complex systems working in concert, and which was therefore highly susceptible to single-point failures which could corrupt the data. On several occasions, such failures were immediately detected by the processing and subsequently corrected. The processing and analysis of the scientific data and the AUV mission logs is expected to continue in a joint effort between the participating institutions over a period of several years.

5.1 Environmental assessment

5.1.1 Seafloor Survey

A substantial number of sidescan surveys were performed over the test area. Figure 11 shows an example of a seafloor map produced using the 390 kHz system, with the position of the TOPAS rail and tower facility and the half-buried sphere S3 identified. The rock outcrop at the Marciana Marina pier access is clearly identified in the top of the image.

A series of stereo photos were taken in the area just beyond C1 and to the left of S3 (as if looking from the rail - see Fig. 4). Two parallel lines of photos were taken, each line conisting of five adjacent positions with 50% overlap. Fig. 12 shows an example of left and right photos from one of the positions. In contrast to observations at the same site during the MCG2-97 experiment, divers reported a lack of defined ripple structure in the experimental area, confirmed by preliminary analysis of the stereo photos. Processing will consist of deriving height fields for each pair of photos, estimation of statistics including two-dimensional spectra, and an effort to create a single mosaic height field from the individual images in order to achieve a better understanding of the larger scale features of the bottom topography.

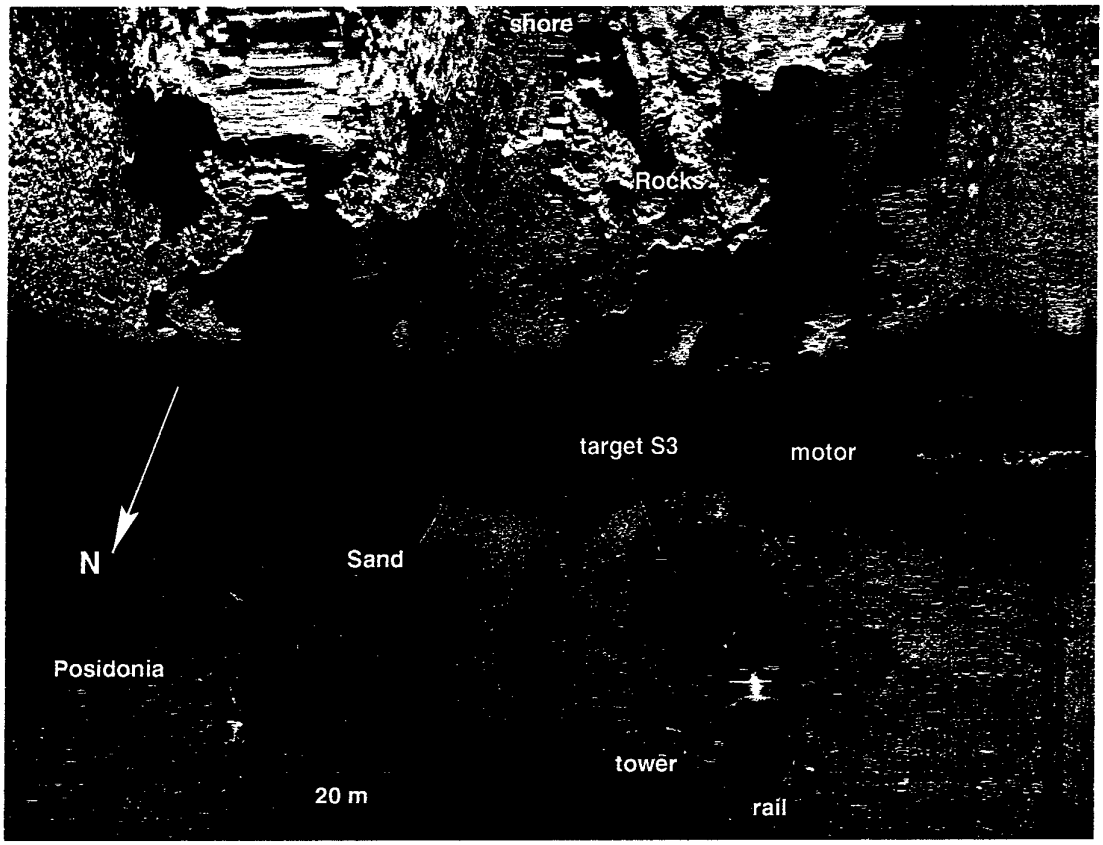

Figure 11 *Sidescan map of test area north of pier access in Marciana Marina. The TOPAS rail and tower facility is easily identified, together with the half-buried spherical target S3.*

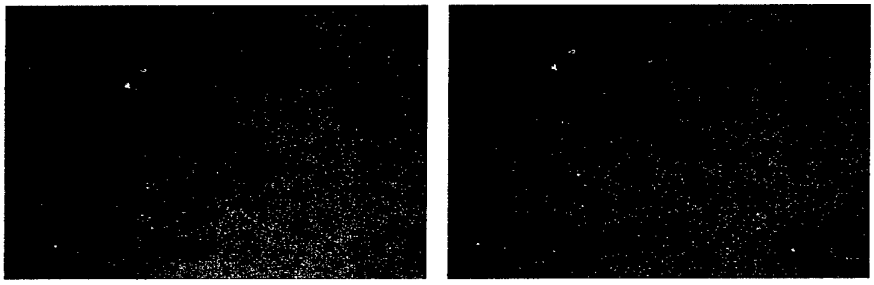

Figure 12 *Example of left and right photos to be used for estimating bottom topography. Approximate size of imaged patch: 650 mm x 450 mm.*

5.1.2 Geophysical Survey

Analysis of the sub-bottom profiling sections indicate a 9 m sediment layer on top of the porphyrite dioritic bedrock. The stratification of the sediments from the flat area near the coast to the steep escarpment is characteristic of a high-energy deposition environment. This suggests a medium-to-large, sand and gravel sediment composition.

Four types of measurements were made on the three core samples collected in the test area. Figure 13 shows the results of the measurements completed at this point on one of the cores collected close to the TOPAS rail.

1. *Magnetic susceptibility:* All the cores highlight a variation of magnetic susceptibility between 5 and 10 cm. This indicates a variation in the sedimentation process due to an unusual event, e.g. a fluvial event with an enrichment of magnetic material or contribution from waves or coastal currents.
2. *Sound Speed:* The sound speed measurements were performed at a frequency of 200 kHz. The results have been processed with two different techniques. The first compares the velocity of the sediments with those of the water sample (on another liner). The second compares the velocity of the sediments with salt water on the upper part of the core, the characteristics of which were measured using a CTD. The three cores have close to identical sound speed profiles.
3. *Grain size:* These measurements were undertaken only on one of the cores, (see grain size distribution of Fig. 13).
4. *Permeability:* These are currently being performed on two of the cores.

5.2 AUV operations

The *Odyssey* AUV was launched and operated from the *Alliance*, anchored approximately 600 m from the target area (Fig. 14). Given the numerous different systems, the launch coordination from the *Alliance* Main Scientific Laboratory (MSL) was critical for which an efficient count-down procedure was developed.

Mission design and implementation comprised several steps. First, the mission track was designed using a graphical tool on a workstation in the MSL (Fig. 15). The mission plan was then translated into a series of way-points between which the AUV would navigate using the long baseline (LBL) acoustic navigation system, at selected depths and speeds. The mission file was downloaded em via the computer network to the vehicle computer. At the same time the acoustic acquisition system was programmed for the mission.

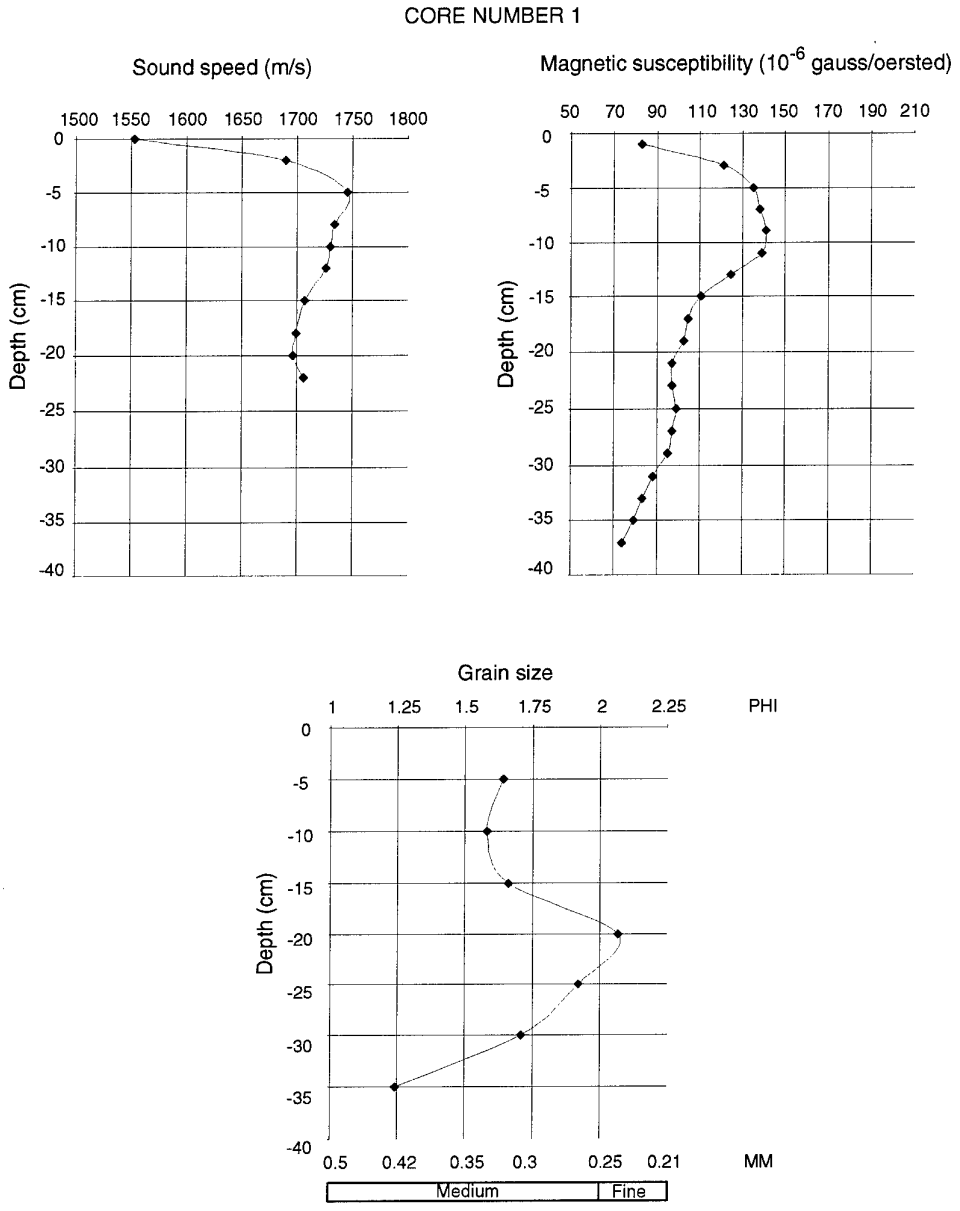

Figure 13 *Sound speed, magnetic susceptibility, and grain size profiles measured on Core No. 1.*

Figure 14 *Launch and recovery of Odyssey AUV from R/V Alliance.*

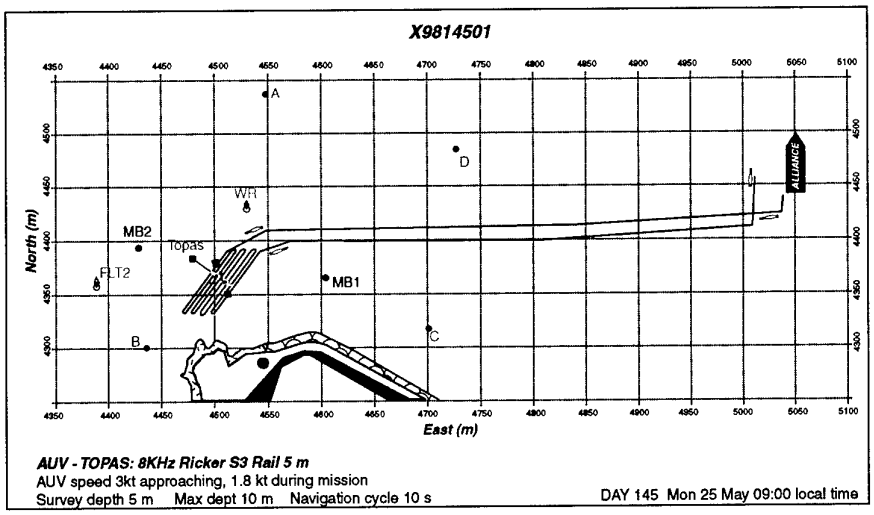

Figure 15 *Survey layout for AUV mission x9814501. The AUV transected to the target area where it used way-point navigation to complete a survey pattern over the target field, measuring both back- and forward scattering produced by insonifying the targets with the TOPAS source. The navigation was performed with a few metres accuracy using an LBL network with 4 transponders, the position of which is indicated by the red markers labeled A-D. The figure shows also the positions of the marker buoys used to delimit the area of the experiment.*

Figure 16 *Odyssey AUV performing acoustic survey with TOPAS insonifying the target field.*

A typical mission would take the AUV from the *Alliance* to the target area at a speed of 3 kn. Once reaching the target area, the AUV would make 8 passes at less than 2 kn back and forth over the targets (Fig. 16). During the survey, the vehicle would initiate an LBL navigation fix every 10 s. The LBL interrogation pulse was measured on the fixed arrays and used to trigger the TOPAS source to perform 7 s of transmissions after a 2 s delay, typically transmitting 3 pulses per second. This procedure eliminated interference between the LBL and the scattering measurements and ensured that all pings in a TOPAS transmission cycle were collected in one data file on the AUV. The first pass would typically pass very close to the TOPAS, measuring target backscatter, with each successive pass displaced 3 m further away, so that the last tracks measured forward scatter off the targets. Once the survey pattern was complete, the AUV would transit back to the *Alliance*. After surfacing approximately 100 m from the *Alliance*, the AUV would be towed back with the work-boat and lifted onto the deck. On deck, the AUV was immediately connected to the computer network, and data was uploaded from the navigation computer and the acoustic acquisition system. The data were then stored on the *Alliance* computers and backed up to optical disks and high density tapes.

The AUV navigation data were processed immediately in order to verify the completion of the mission plan, and for parsing of the reduced navigation data with the acoustic data. An example of post-mission navigation results is shown in Fig. 17.

Thirty-nine AUV missions were launched and completed, totaling 14 hours of submerged time. The performance of the AUV was completely reliable, and no serious hardware problems were encountered. The control algorithms developed at MIT were capable of repeatedly performing the desired survey patterns in the target area with a navigation accuracy of a few metres using the LBL acoustic net deployed in the area. As discussed later, a significant 'along track' navigation bias was observed on the inbound legs in the vicinity of the TOPAS tower, the cause of which is still

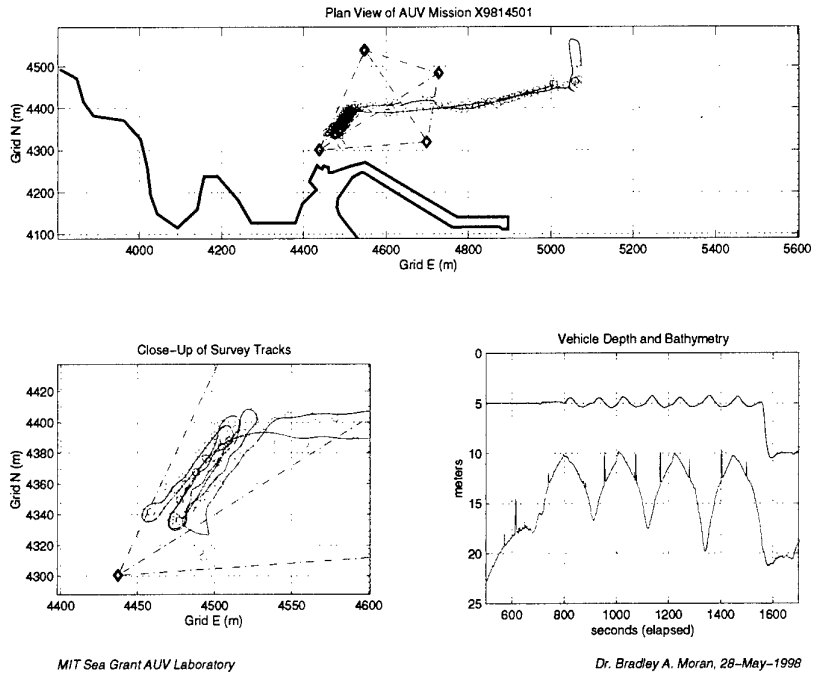

Figure 17 *Long-baseline navigation fixes for mission x9814501. The upper frame shows the full mission track, while the lower left shows the navigation fixes for the survey portion over the target area. The red circles indicate the positions determined directly from the LBL, while the blue line shows the position estimate resulting from a combination of the LBL and dead-reckoning. The lower right frame shows the depth history of the AUV as a blue curve, and the altimeter reading as the green curve. The survey depth was 5 m, but the vehicle had a 7 m bottom envelope, yielding the wave pattern in the actual survey depth. Note also the spikes associated with the AUV passing over the HLA.*

being investigated. Despite this problem, the 'cross track' navigational performance during the later part of the experiment became sufficiently reliable to allow routine AUV navigation to within a 5 m stand-off distance of the TOPAS tower.

To facilitate fusion of the acoustic and non-acoustic measurements, a local (UTM) coordinate system was established for the experiment, defined as having

$$[(x, y) = (5000\text{m}, 5000\text{m})] \sim [42°49'.00\text{N}, 10°12'.00\text{E}]$$

This particular choice was made to make all local coordinates positive.

5.3 AUV self-noise

The 'swordfish' array with its autonomous data acquisition system, provided a means of determining the AUV's self-noise contributions at the array during vehicle operation at sea. Examples of these self-noise computations, at nominal vehicle speeds of 2 and 3 kn, are shown in Figs. 18 and 19. In both figures, the left-hand frames show the periodogram analysis of the 8 array channels, with channel 8 being the closest to the vehicle nose. The frequency axis spans acoustic frequencies up to the design frequency of the array (7.5 kHz). The right-hand frames show the results of wavenumber-frequency transformation; the abscissa indicates the propagating wave numbers across the array, such that all physical acoustic arrivals at the array are confined to a central v-shaped region in the wave number - frequency plane. The radiated self noise from aft of the vehicle is seen at negative wave numbers, projected along the left-hand edge of the v-shaped region (aft end fire).

The vehicle self-noise was less intrusive than expected. The acoustic decoupling provided by the array mounting and the location of the array on the nose of the vehicle contributed to limiting the effects of self-noise. More importantly, however, the vehicle was slowed to 2 kn during acoustic acquisition with consequent reduction in overall noise output from the thrusters (as can be seen by comparing Figs. 18 and 19). Furthermore, the frequency regime of the acoustic transmissions from the parametric source were generally above the major components of vehicle self-noise (as evidenced by the TOPAS transmission in Fig. 19 seen along the right-hand side of the v-shaped region (forward end-fire)).

The ability to monitor vehicle noise emissions during operations at sea is likely to prove an important aid to improving the self-noise characteristics of the next generation of AUV's, currently under consideration at MIT.

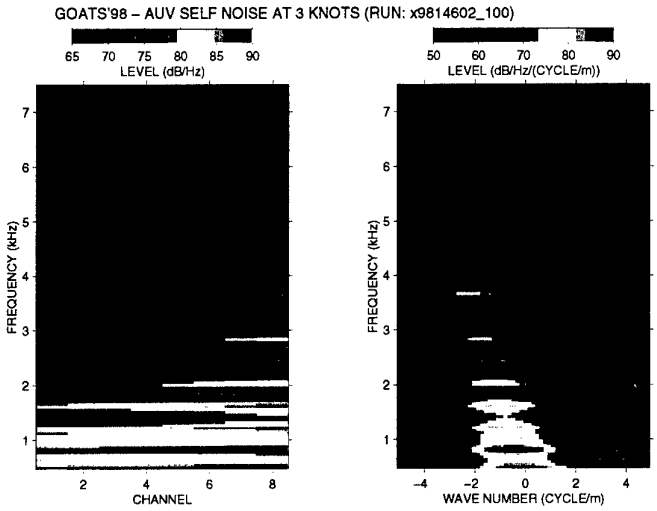

Figure 18 *AUV self-noise measurement for cruising speed 3 kn. Left frame shows a periodogram versus channel, with channel 1 being at the tip of the array. Right frame shows the corresponding wavenumber-frequency ($f-k$) diagram, with negative wavenumbers corresponding to signals coming from the AUV.*

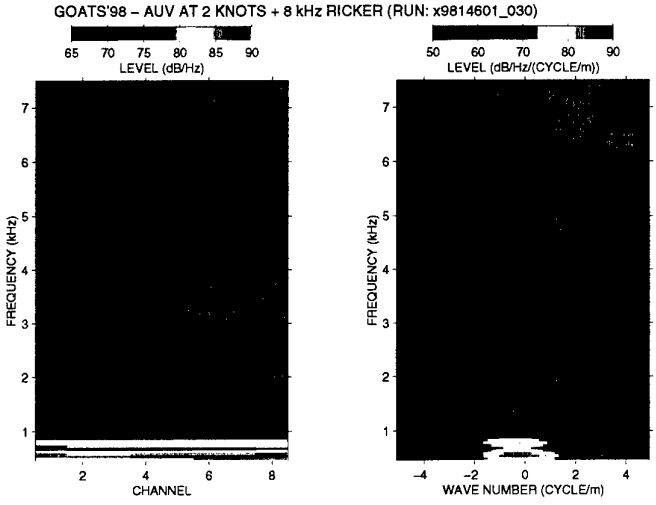

Figure 19 *AUV self-noise measurement during survey at 2 kn speed. Left frame shows a periodogram versus channel, with channel 1 being at the tip of the array. Right frame shows the corresponding wavenumber-frequency ($f-k$) diagram, with negative wavenumbers corresponding to signals coming from the AUV. Energy in forward beam is due to TOPAS transmissions.*

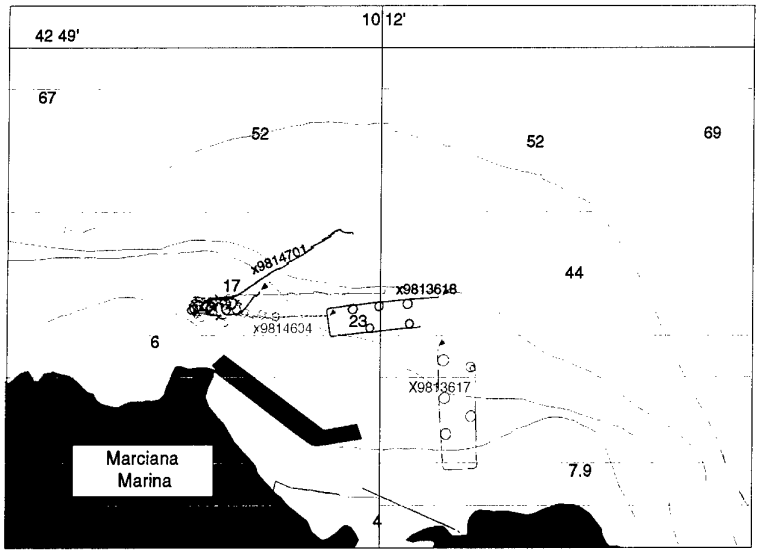

Figure 20 *Tracks of the four missions undertaken by the AUV with echosounder.*

5.4 AUV echosounder surveys

By keeping the AUV altitude to less than 5 m, the source and receiver were effectively in a bistatic geometry. Choosing the AUV tracks to consist of circular sections connected by straight line sections, anisotropic aspects of the seabed would be sensed. Fig. 20 shows the track plots of the four missions undertaken during the experiment. Only a small portion of run x9813617 has been partially processed. Fig. 21 shows a contour plot of the normalized echo envelope for the first 160 s of the mission *vs* time and echo delay. Fig. 22 shows the corresponding normalized, integrated echo envelope along the dead-reckoned vehicle track for this portion of the mission. Both figures show the results for the two echosounder frequencies, 8 and 16 kHz, normalized individually.

The echo delay in Fig. 21 refers to the first arrival from the bottom. The AUV was programmed to maintain a constant altitude of 4 m above the bottom. The variation in the echo delay is associated with the deviation from the desired bottom-following track, as confirmed by the vehicle altimeter reading for the same period shown in the second frame of Fig. 23. This figure also shows the corresponding vehicle roll and pitch. The echosounder cone clearly has an effect on the control of the AUV. On the other hand, the resulting track deviation is less than one metre, in spite of the significant change in the vehicle hydrodynamics imposed by the echosounder cone.

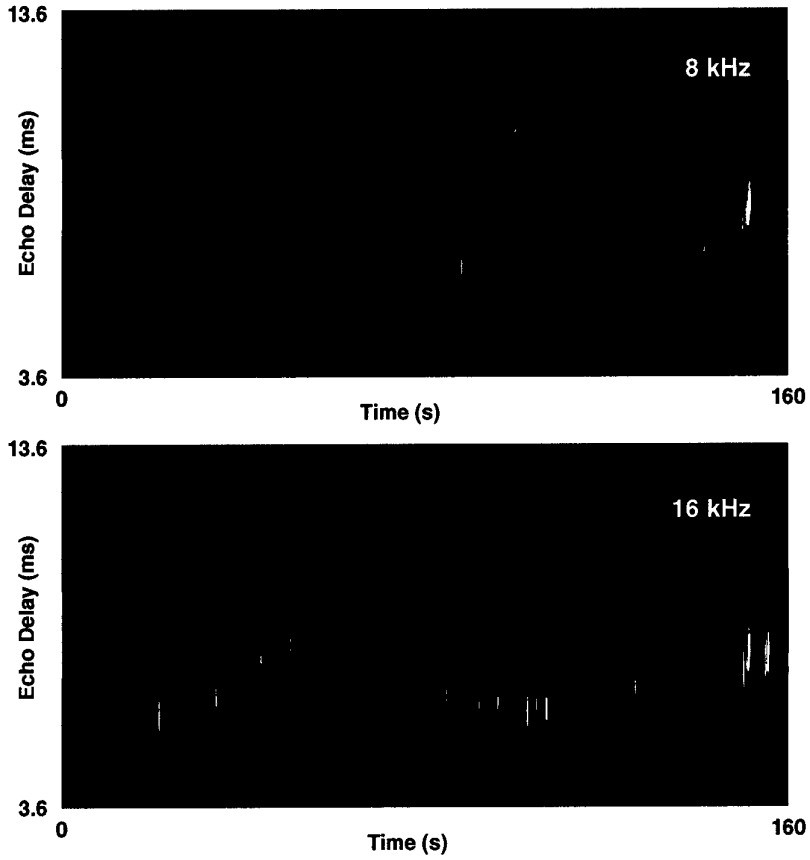

Figure 21 *Echo amplitude, normalized but uncorrected for vehicle motion, measured during portion of mission* x9813617. *Vertical axis represents the echo delay, while the horizontal axis indicates mission time.*

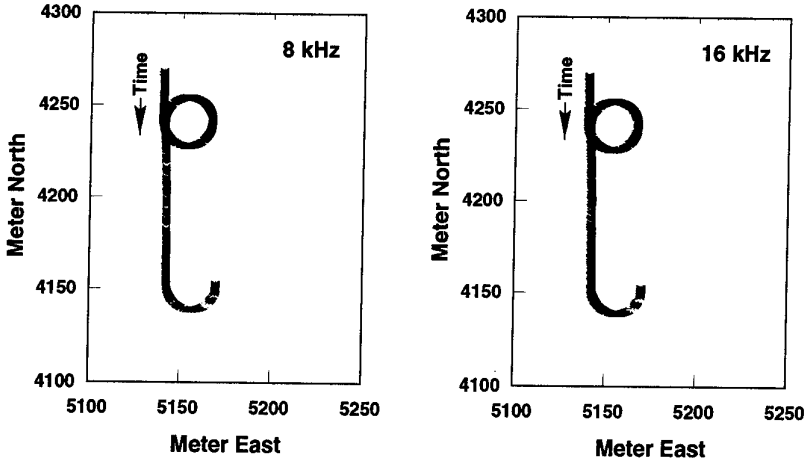

Figure 22 *Portion of mission* x9813617 *colored with normalized, integrated echo amplitude at 8 kHz and 16 kHz, corresponding to results shown in Fig. 21. These preliminary results are uncorrected for vehicle motion.*

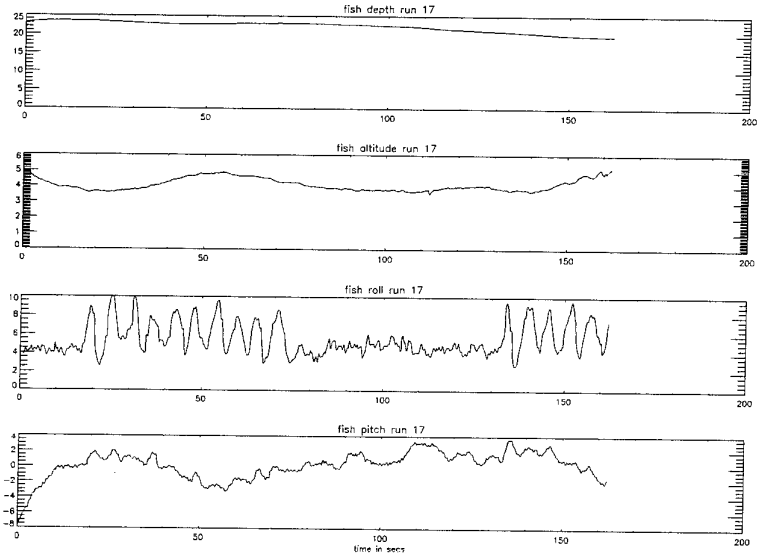

Figure 23 *AUV motion during portion of mission* x9813617 *shown in Fig. 22. From the top, the frames show AUV depth, altimeter reading, vehicle roll, and vehicle pitch.*

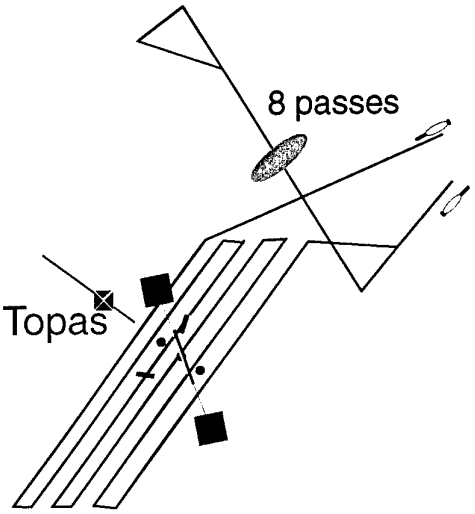

Figure 24 *AUV track for run x9814601.*

5.5 TOPAS replicas

Due to the constraints imposed by the nature of the parametric transmitter (i.e. it requires a minimum distance of approximately 30 m to form the endfire beam) and by the shallow waters where TOPAS experiments were performed in the past, good replicas of the linear frequency modulated pulses (LFM) have not been recorded. Either the surface or the bottom reflections have always contaminated the reception of the direct transmission when the signal was longer than 1ms.

The maneuverability of the AUV was exploited to collect a set of replicas of the TOPAS transmissions. At the end of a standard target run (x9814601), the TOPAS transmitter was rotated towards the open sea and tilted in the vertical half way between the surface and the bottom, while the AUV was programmed to repeat 8 passes at mid water depth at a distance of 50 m from the tower (Fig. 24). During each run, the TOPAS transmitted a LFM pulse with different time and bandwidth parameters, and the signal was received on the 8-element array.

Figure 25 shows an example of a received LFM, with its spectrum and the matched filter output using an ideal synthetic replica. The matched filter output shows that the interference with the surface and/or the bottom has been minimized, with only a small surface reflection still present. If necessary, this will be removed by cepstral processing methods.

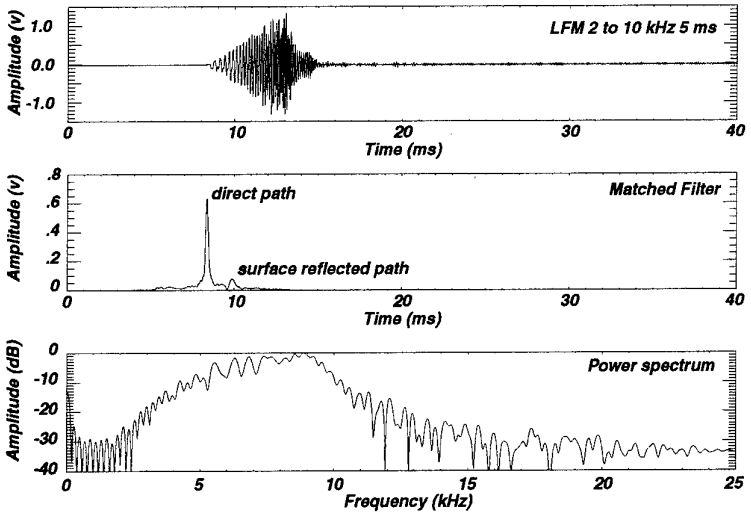

Figure 25 *Signal received on one hydrophone of the AUV during run x9814601. The spectrum and the matched filter output using an ideal synthetic replica show only a small surface reflection following the direct arrival.*

5.6 Scattering and Reverberation - Fixed Arrays

For measuring backscattering from the targets and reverberation with the fixed arrays (vertical 16-element array and 128-element horizontal array), the tower was moved to a given position on the rail. Then, the main response axis of the TOPAS transmitter was trained on a section of the bottom with the pan and tilt motors, a series of pulses was transmitted, and the return signals recorded. Each target was measured over a range of grazing angles including above and below the nominal critical angle. The following two sections will show brief examples of data taken with these two arrays. A further section will describe data taken on the buried hydrophone array with the shotgun seismic source.

5.6.1 Vertical Line Array

Figure 26 shows an example of the time series recorded on the 16 channels of the vertically mounted receive array. Channel number one is physically the bottom-most channel in the array, and channel 16 the top-most . Note that channel 11 was not functioning. In this case, the TOPAS was trained on S2 with a nominal grazing angle of 27°, and the transmit pulse was a Ricker wavelet. This transmit pulse is broadband (significant source levels in the range 2–16 kHz), and has time-bandwidth product close to one. For this geometry, the expected time of arrival for

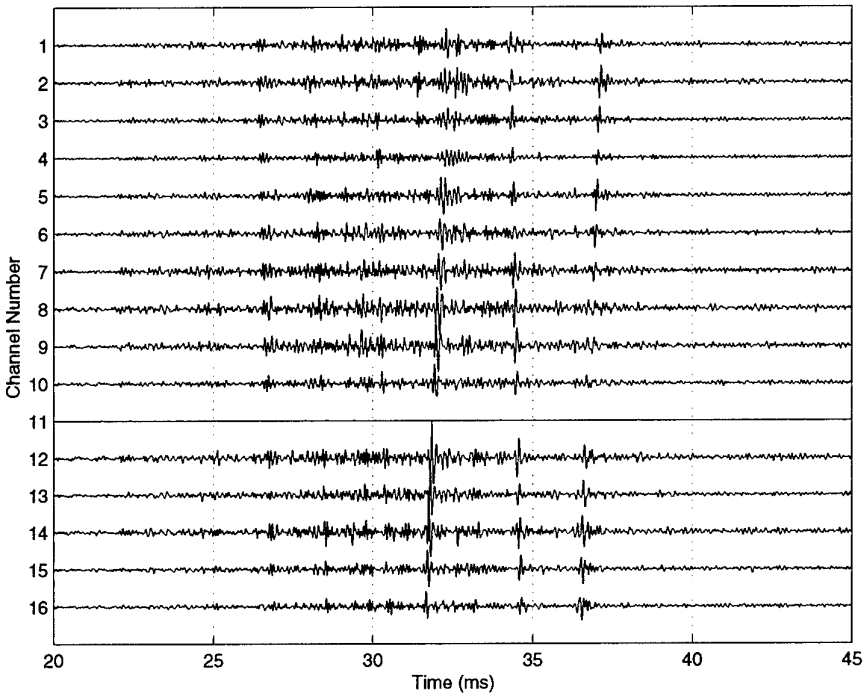

Figure 26 *Example of data taken on 16-element vertical array: direct S2 arrival at ~28.8 ms, surface S2 arrival at ~32–33 ms, direct S3 arrival at ~34.8 ms, and surface S3 arrival at ~36–37 ms.*

the reflection from S2 is roughly 28.8 ms. It is difficult to discern a definite return on the individual hydrophone time series corresponding to this 'direct' S2 arrival. The strong return on each channel between roughly 32 and 33 ms is due to energy that has scattered from S2 up to the surface and then to the receive array. We refer to this as the 'surface' S2 arrival. The beam of the TOPAS was wide enough to also insonify S3, and the direct arrival can be seen across the array at roughly 34.8 ms. The surface S3 arrival can also be seen between roughly 36 and 37 ms across the array.

By using conventional plane-wave beamforming and mapping the beams into range-depth space, an image can be formed of the location of the scattering centers in the vertical plane. Figure 27 shows the results for the data shown in Fig. 26. The source-receiver combination is located at coordinate (0,0) in this plot. The tower height was 10 m, hence the insonified portion of the bottom can be seen to be mapped out at a depth of -10 m. The nominal *plan range* (i.e., the distance along the bottom measured from the point directly below the source) for S2 is 19.5 m, and 24.5 m for S3.

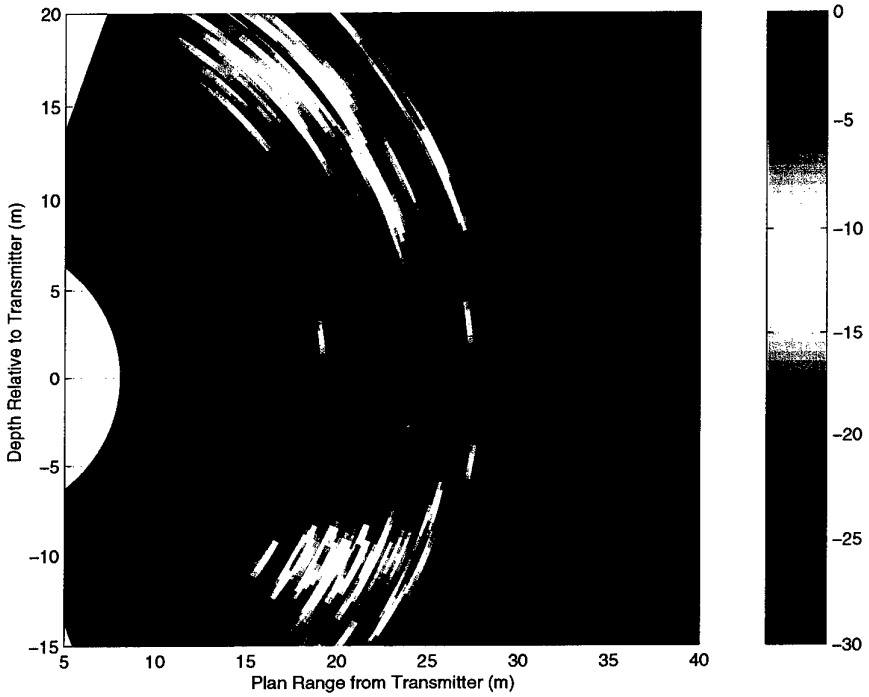

Figure 27 *Data from 16-element array: results of beamforming and mapping into range-depth space. The nominal plan range is 19.5 m for S2 and 24.5 m for S3.*

It is interesting to note the high scattered levels mapped at an apparent depth of +15 m due to surface arrivals from the targets and bottom reverberators. The two highest peaks are due to scattering from S2 and S3 and are commonly referred to as 'image' returns. In this example, the image of S2 appears to have higher signal-to-reverberation ratio than the direct return.

5.6.2 Horizontal Line Array

As mentioned previously, the 128-element horizontal line array was used in two configurations. The first simulated a monostatic geometry, in which the array was placed at the end of the rail closest to the target field, and oriented perpendicularly to the rail. This position was used to gather data over a long physical aperture in order to see how forming narrow beams could increase signal-to-reverberation ratio for detection of buried objects. Figure 28 shows an example from this configuration. Here the TOPAS was pointing to target S3. Every fourth channel on the array is displayed. Due to trigger problems on playback, the time scale is in relative, not absolute, milliseconds. The direct transmit signal can be seen across the array at 80 ms on the plot. The direct and surface returns of S3 can be seen at roughly 104.5 and 110 ms, respectively.

In the second configuration, the array was deployed over the target field in order to measure the bistatic scattering characteristics of the targets. Figure 29 shows an example of data collected on the horizontal array in the bistatic configuration. Here the TOPAS was pointing to target S2. Again, only every fourth channel is displayed. The first signal on each element (arrival time varies from roughly 20 to 26 ms across the array) is the direct transmit pulse. The second signal (arrival time varies from roughly 22 to 27.5 ms across the array) is believed to be due to scattering from the motor on the end of the rail used for moving the tower. The last obvious signal on each channel (arrival time varies from roughly 33.5 to 29.5 ms across the array) is the reflection from S3. From geometrical and travel time considerations, the return from S2 should be arriving at roughly 27 ms near the center of the array, and roughly 29 ms at the ends of the array. Further processing will be necessary (sub-array and focused beamforming) in order to more clearly describe this data.

5.6.3 Buried Hydrophone Array

Figure 30 shows an example of data taken on the buried hydrophone array during a firing of the shotgun seismic source. Hydrophone numbers 12 and 13 were on the metal rod closest to the source, and numbers 0 and 1 were furthest away. Hydrophone number 5 was in the water column. The first arrival on all hydrophones is the direct (compressional wave) pulse, and the second arrival is due to the surface

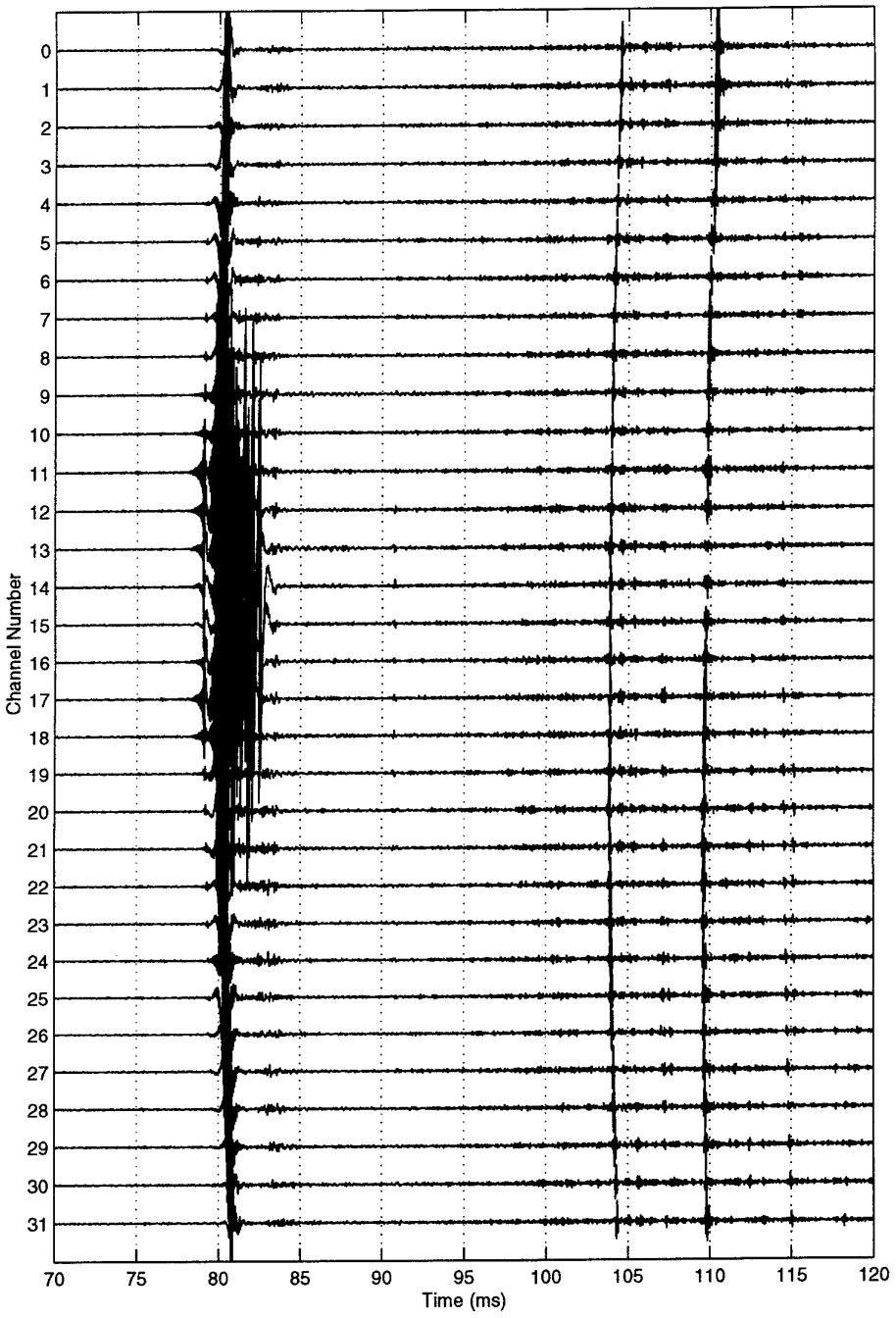

Figure 28 *Example of 128-element array data in monostatic configuration (every fourth channel displayed). The direct transmit pulse appears at ~80 ms, direct S3 arrival at ~104.5 ms, and surface S3 arrival at ~110 ms.*

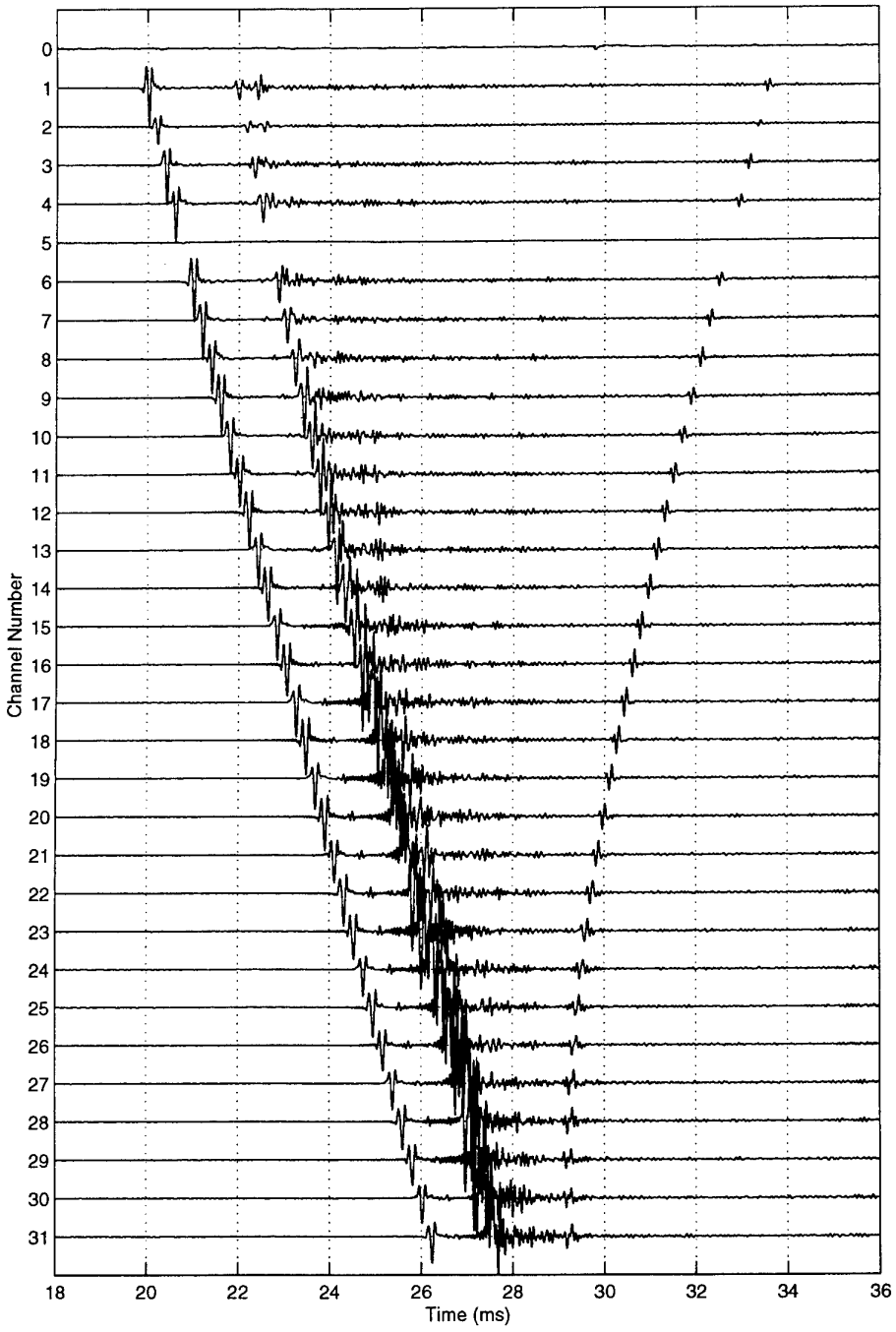

Figure 29 *Example of 128-element array data in bistatic configuration (every fourth channel displayed). The direct transmit pulse appears from ~20–26 ms across the array. The large signal at ~22–27.5 ms is believed to be due to scattering from the motor used to move the tower on the rail. The direct S3 arrival appears between 33.5 and 29.5 ms across the array.*

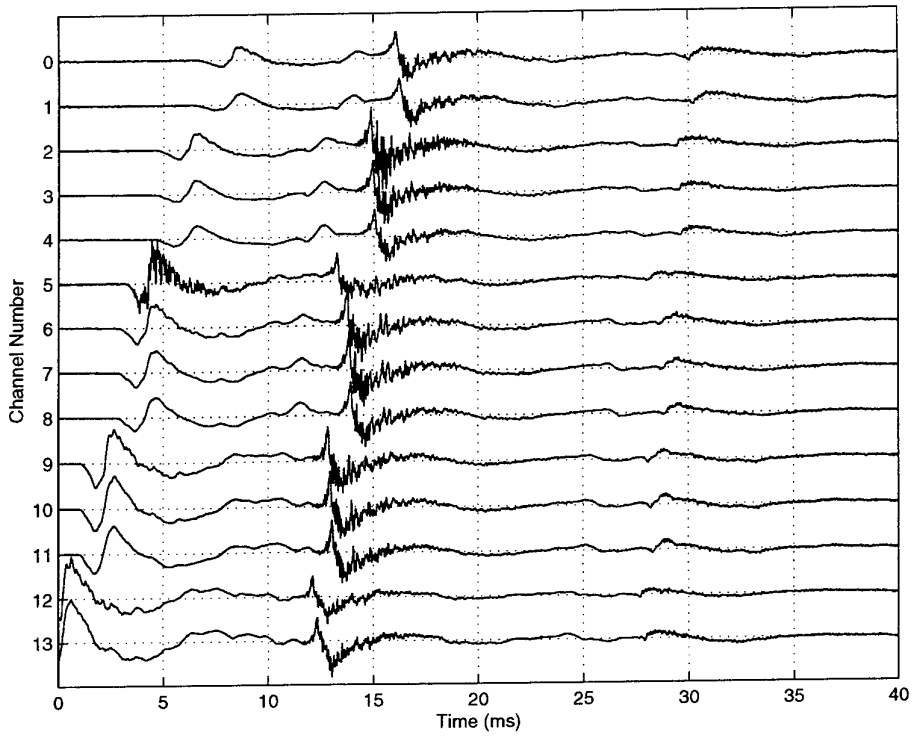

Figure 30 *Example of shotgun seismic source data on buried hydrophone array. The direct compressional wave arrival appears between 0 and ~10 ms across the array, and the surface arrival appears between ~11–19 ms across the array.*

bounce of this pulse. Further processing of this data will involve determination of any direct shear wave pulses, and of target echoes due to either compressional or shear wave excitation.

5.7 Scattering and reverberation - AUV array

A total of more than 30 Gbyte of acoustic data was collected by the array and acquisition system on the AUV during 15 survey missions over the target field insonified by the TOPAS. All the missions consisted of survey tracks similar to the one shown in Fig. 15, although the detailed survey pattern was refined throughout the experiment to optimally sample the back and forward scattered field by all the targets at various incident angles.

To avoid interference between the LBL navigation system and the TOPAS, and to facilitate the fusion of the acoustic data with the AUV navigation, a special navigation/acquisition cycle was designed, with the TOPAS transmissions being

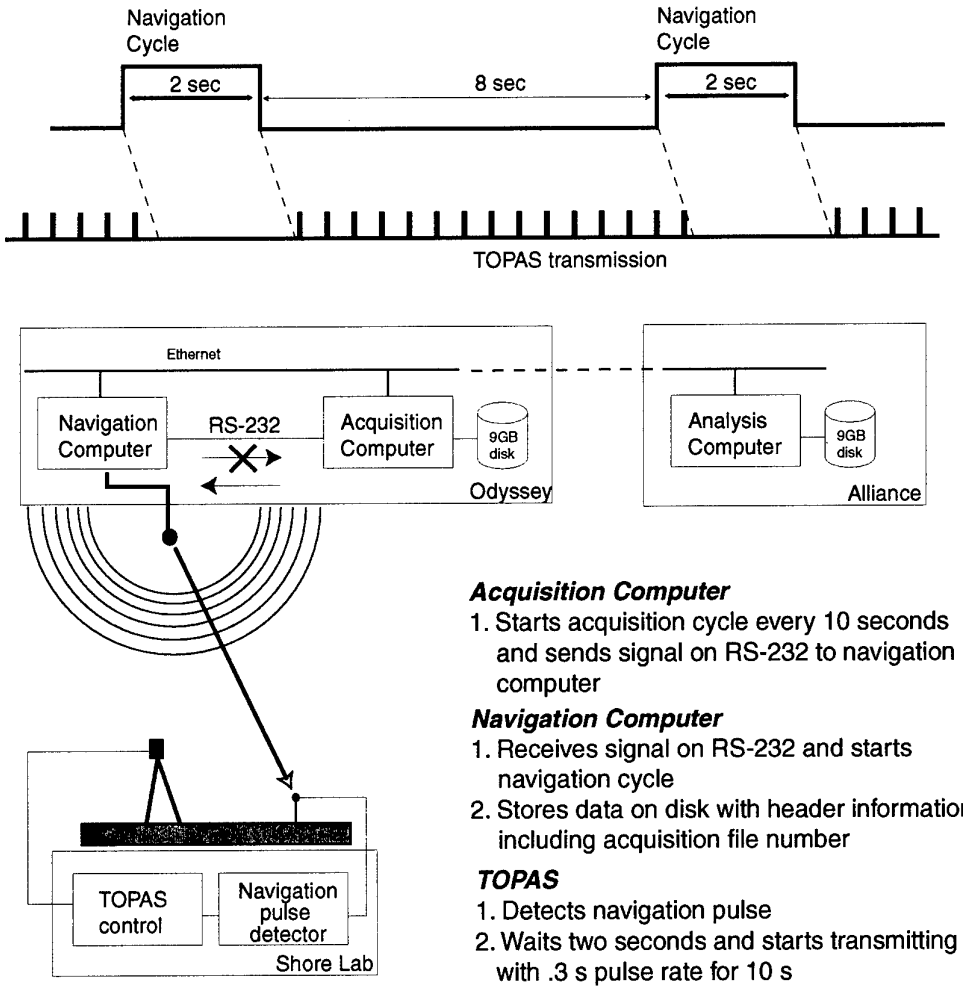

Acquisition Computer

1. Starts acquisition cycle every 10 seconds and sends signal on RS-232 to navigation computer

Navigation Computer

1. Receives signal on RS-232 and starts navigation cycle
2. Stores data on disk with header information including acquisition file number

TOPAS

1. Detects navigation pulse
2. Waits two seconds and starts transmitting with .3 s pulse rate for 10 s

Analysis computer

1. Connects to AUV LAN and reads data from acquisition computer disk
2. Reads header from navigation computer
3. Performs beamforming and data quality analysis

Figure 31 *Time synchronization of LBL navigation, TOPAS transmissions and acoustic data acquisition on AUV.*

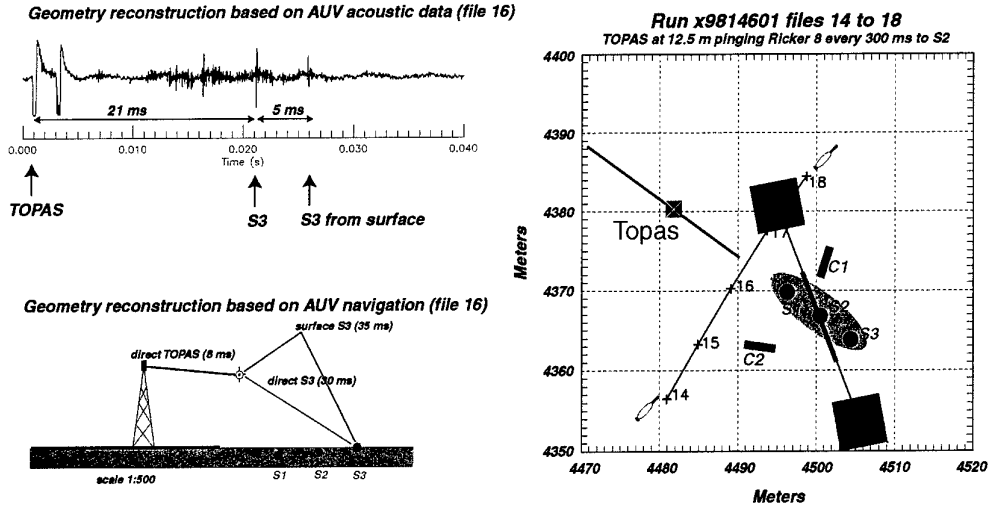

Figure 32 *Geometry reconstruction of run x9814601 based on AUV navigation and acoustic data*

triggered by the LBL navigation (see Fig. 31). The 10 s cycle was controlled by the AUV acquisition computer, which started the sequence by instructing the navigation computer that a new 10 s data file was being initiated, in response to which the AUV controller would initiate an LBL navigation cycle and store the acquisition file identifier in the vehicle log. The LBL interrogation pulse from the AUV was detected by a TOPAS receiver, initiating a 2 s delayed trigger of the TOPAS source which was aimed at a particular target. After this delay, the TOPAS would transmit a sequence of Ricker wavelets or LFM sweeps at a rate of 0.5 - 3 per second, for a total of 8 s. The AUV acquisition system would then initiate a new cycle. Following each mission, the acoustic data would be downloaded to the *Alliance's* computer system, fused with the navigation data, and backed up on optical disks and tapes, using the data structure described in Sec. 4.6.

5.7.1 Micro-navigation and synchronization

To check the quality of the acoustic scattering and reverberation data and to validate the experiment geometry, the direct TOPAS signal and the targets' surface and bottom multiples were used to navigate the position of the TOPAS transmitter relative to the AUV. Figure 32 shows one hydrophone of the 8 element array mounted on the AUV at the point of closest approach to the TOPAS rail during one of the survey legs of mission *x9814601* (file 16). The frame to the right shows the track of the AUV as it was estimated by the LBL navigation system, indicating the sections

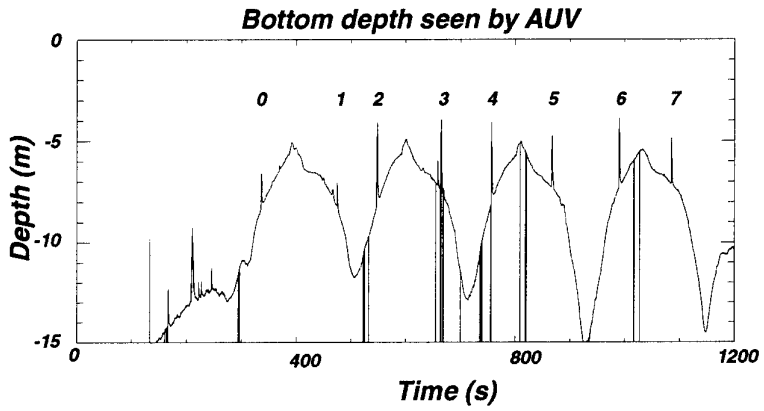

Figure 33 *AUV altimeter data showing passages over 128 element horizontal array during mission* x9814501

covered by each acoustic data file collected by the AUV. The position of the TOPAS tower, rail and target field is based on measurements performed by the divers during deployment. The bottom frame to the left shows the geometry for data file 16 in the vertical plane, along the rail-target axis. The geometry reconstruction based on AUV navigation predicts that the direct arrival from targets S2 and S3 should arrive 17 and 22 ms later than the direct TOPAS transmission, and that the S3 surface reflected path should arrive 5 ms after the direct echo. The acoustic data shows good agreement as the direct paths arrive 16 and 21ms after the direct TOPAS transmission, and the S3 surface reflected path arrives 5 ms after the direct echo. The S2 surface reflected path is masked by the S3 direct echo.

Another way to check the AUV navigation was to use the AUV altimeter data when passing over the 128 element horizontal array suspended over the target field. Figure 33 shows the altimeter data during mission x9814501. Clearly evident are the sudden changes of bottom depth as measured by the AUV altimeter, corresponding to the moment the AUV was passing over the array.

Figure 34 shows the AUV track for the same run superimposed on the geometry of the TOPAS rail and target field, as measured by the divers. The white circles indicate the positions of the passage over the array as measured by the AUV altimeter. It was found that for outbound AUV tracks (i.e. tracks going from shore to the open sea) the agreement between AUV navigation and the experimental geometry measured by the divers was quite good (less than 2 m error), but many of the incoming tracks are offset by more than 10 m. This seems to indicate a bias in the LBL navigation of the AUV, that will have to be further investigated.

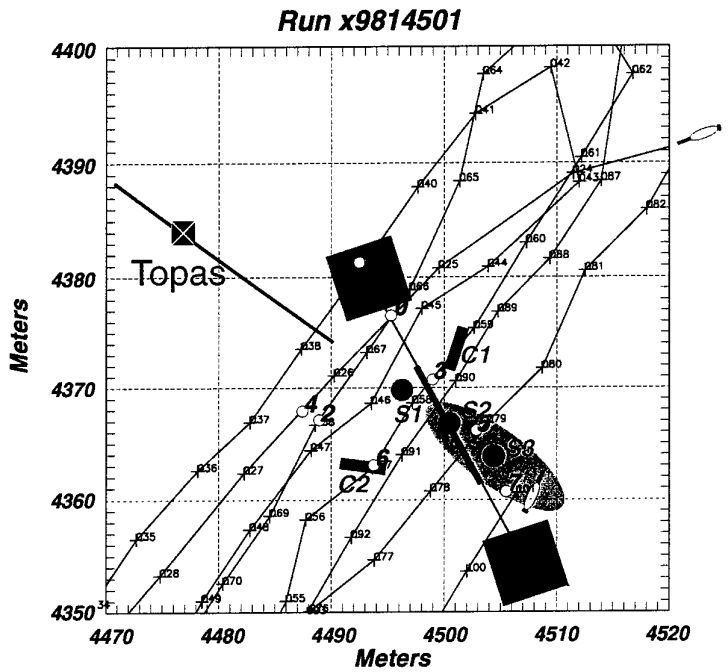

Figure 34 *A UV passage over the target area during mission* X9814501. *The black lines indicate the LBL navigated survey track, while the white circles indicate the altimeter detections of the 128-element HLA.*

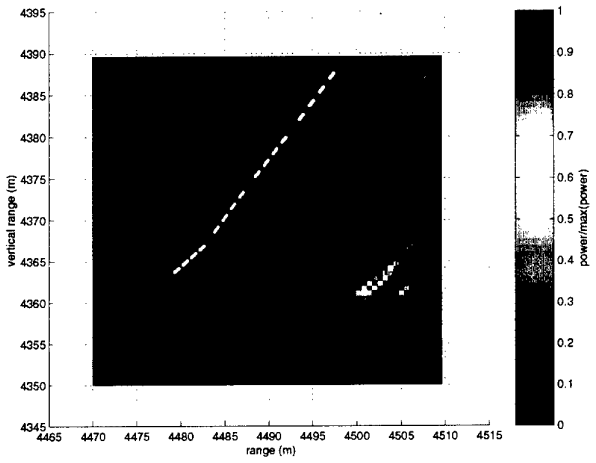

Figure 35 *Bistatic imaging of target area using data (files 36-40) recorded during the first outbound leg of mission x9814501, shown in Fig. 34. This same acoustic data was used for micro-navigating the TOPAS facility relative to the LBL fixes for the AUV, and the target S3 is well imaged except for an offset associated with an uncertainty in direction of the TOPAS rail.*

5.7.2 Bistatic imaging

The time series recorded on the swordfish array of the AUV were combined with the LBL navigation to obtain incoherent images of scatterers in the target field. Here some preliminary results are shown for data recorded during mission x9814501. Figure 35 shows the results of the imaging for a pass of the AUV between the TOPAS tower and the target field recorded in files 036 through 040. Superimposed on the image are the best estimates of the TOPAS tower and rail position as estimated by the micro-navigation procedure discussed in the previous section. The yellow dots lie along the navigation track of the pass and represent the bistatic receiver positions on all eight elements of the swordfish array, for the twenty acquisitions included in the aperture. These twenty acquisitions are obtained from five distinct TOPAS interrogation sequences, as described in Section 5.2. These interrogation sequences are triggered by the LBL network and have a duration of 10 s. During this time, the TOPAS operates for 7 s. In this experiment the TOPAS transmitted Ricker source pulses with an 8 kHz centre frequency, towards target S3 (the partially buried sphere) from the 5 m rail position. A 0.3 s repetition rate was maintained during the 7 s of TOPAS operation. Of the twenty-four TOPAS transmissions available from each sequence, every seventh was selected for inclusion in the imaging process, yielding a decimated repetition rate of 2.1 s. Thus the yellow dots in Fig. 35 can be seen to lie

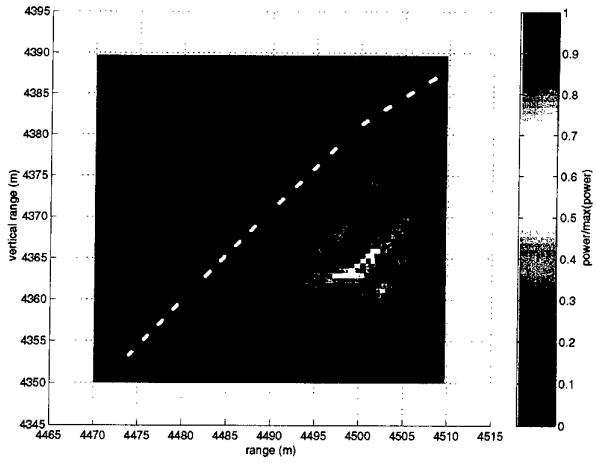

Figure 36 *Bistatic imaging of target area using data (files 23-27) recorded during the first inbound leg of mission x9814501. Although this track did not show the 8 meter bias associated with the other inbound legs, there is still residual bias in the target localization due to inconsistencies in the LBL navigation between files 023-027 and the files 036-040 used for the micro-navigation.*

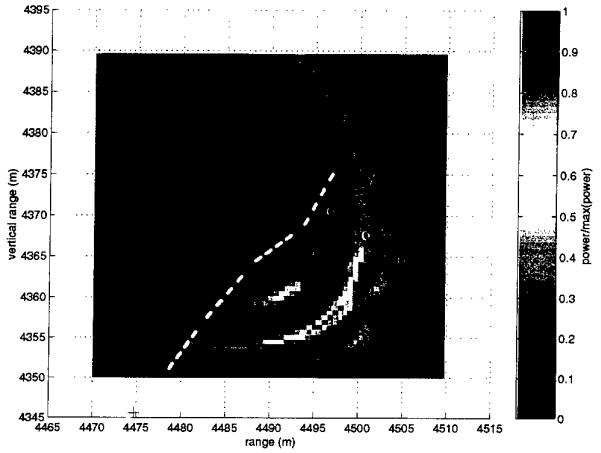

Figure 37 *Bistatic imaging of target area using data (files 45-49) recorded during the second inbound leg of mission x9814501. This image clearly shows a shift in apparent target position due to the bias in the LBL navigation consistently observed during most inbound legs. However, this image is unique in also showing a probable detection of the flush-buried target S2.*

along distinct swordfish array apertures, with the mean distance between apertures determined by the 2.1 s repetition rate and the speed of the AUV (approximately 0.75 m per s during this part of the experiment.) As each TOPAS transmission was recorded on all eight elements of the swordfish array, 160 time series were used in the construction of the image.

The image shown in Fig. 35 is obtained through a process of incoherent time domain beam-forming. For each position in the AUV aperture trajectory, a time domain replica of the reverberation from every hypothetical location in the target field is calculated. The replicas are obtained under the assumption that the reflections from the hypothetical targets consist only of a direct reflection and the first surface bounce. This hypothesis was motivated by the observed structure of the reverberation (see for instance Fig. 34,) which showed only two arrivals for reflections from strong scatterers such as the partially buried sphere S3. Replicas were calculated in reduced time, i.e., time after direct blast, due to the characteristics of the data set, which will be discussed below. In the examples shown here, the replicas were calculated for a Ricker wavelet with an 8 kHz centre frequency, band passed between 2 and 5 kHz, to reduce the resolution required of the imaging algorithm, and to reduce sensitivity to navigation errors. The replicas were obtained for hypothetical scatterer depths of 12.5 m, a TOPAS source depth of 5.0 m, a constant sound speed of 1520 m/s, for the X, Y and Z location of each receiver in the aperture, and for the hypothetical [x,y] scatterer positions shown in the image.

The replicas were calculated using the source pulse of the TOPAS in reduced time. The reduced time approach was necessary due to the unsynchronized nature of the individual TOPAS transmissions. As the data recorded on the AUV swordfish array from one TOPAS interrogation to the next were without a common time basis, the data must be reduced to a common time basis through the selection of the direct arrival from the TOPAS transmitter to the swordfish array. This process, laborious and subject to human error, reduced the potential resolution which could be obtained with bistatic imaging in cases where accurate triggering and a common time basis between the TOPAS transmitter and the AUV were available. However, in the presence of significant navigational uncertainty, the resolution degradation introduced by the selection procedure is believed to be of little consequence.

The image is obtained by taking the inner product of the envelope of the replica time series with the envelope of the band passed time series for every receiver in the aperture, and summing over the number of contributing receivers in the aperture. The envelopes are obtained as the magnitude of quadrature components consisting of the time series and its Hilbert transform. If a single element in the aperture is used, then the ambiguity function is an ellipse, the major axis of which connects the source and the receiver location. As additional receivers are added, the ellipses tend to constructively add at the true scatterer location on the original ellipse. The sidelobes of this incoherent processing method are very high, as there is no construc-

tive/destructive interference which can reduce(in relative terms) the returns from incorrect locations on the ellipse. However, it is felt that the approach represents a good first step in dealing with a data set with significant navigational uncertainty.

As discussed in the previous section, the navigation of the AUV position is significantly biased. This is a result of both the difficulties in using acoustic arrivals to navigate in a fading, multipath environment and to uncertainty in the position of the LBL transponders in relation to the TOPAS rail. The micro-navigation procedure was used to fine tune the navigation for files 036 through 040 of the x9814501 data set, with the result that the image shown in Fig. 35 quite accurately locates target S3, which was the target of opportunity used during the micro-navigation procedure. Observation of the result shows that the target is located better in range than in azimuth and that there are false images in front of and behind the true target location. These false images are present for single scatterers and are part of the ambiguity function for the incoherent time domain beamformer used in this study. The false images are caused by the two-arrival model for target scattering. When a position slightly closer than the true target location is hypothesized, the replica time series which are generated contain a surface reflected return which arrives at the same time as the direct reflection in the data set. For hypothetical positions on the far side of the target, the direct arrival in the replica time series arrives at the same time as the surface reflection of the actual target. Thus the false returns seen in Fig. 35 are a result of how the replica functions are used to obtain the image.

When the micro-navigated TOPAS rail and target field positions are used self consistently, Fig. 35 shows that good target imaging results can be obtained. In Figs. 36 and 37, the micro-navigation from files 036 through 040 is used for the AUV tracks associated with files 023-027 and 045-049, to see how the performance is affected. In the previous section, it was found through the use of the AUV altimeter that the navigation for most of the 'inbound' tracks of experiment x9815401 suffered 8 m bias of unknown cause, but that inbound files 023-027 were not affected. This is clearly evident from Fig. 36 where the cross track position of the peak of the image, for data files 023-027, closely corresponds to the actual target location. However, the range of the maximum image output is closer than the micro-navigated target position. This indicates that there are residual positional inaccuracies between the navigation for files 036-040 and files 023-027.

In Fig. 37, the last inbound leg imaged for files 045-049, the 8 m positional bias is clearly seen. However, this image is the only one of the three to show a clear return from the flush buried target S2. The stacked time series in Fig. 38 clearly shows the earlier return from S2, which is most clearly visible near the centre of the aperture. The ability of the AUV to pick up the return from the flush buried target during this run is enhanced by the high bistatic angle at which the buried target is observed in the vicinity of the closest point of approach. This result serves as an indicator to the types of gains which can be obtained with bistatic source-receiver configurations.

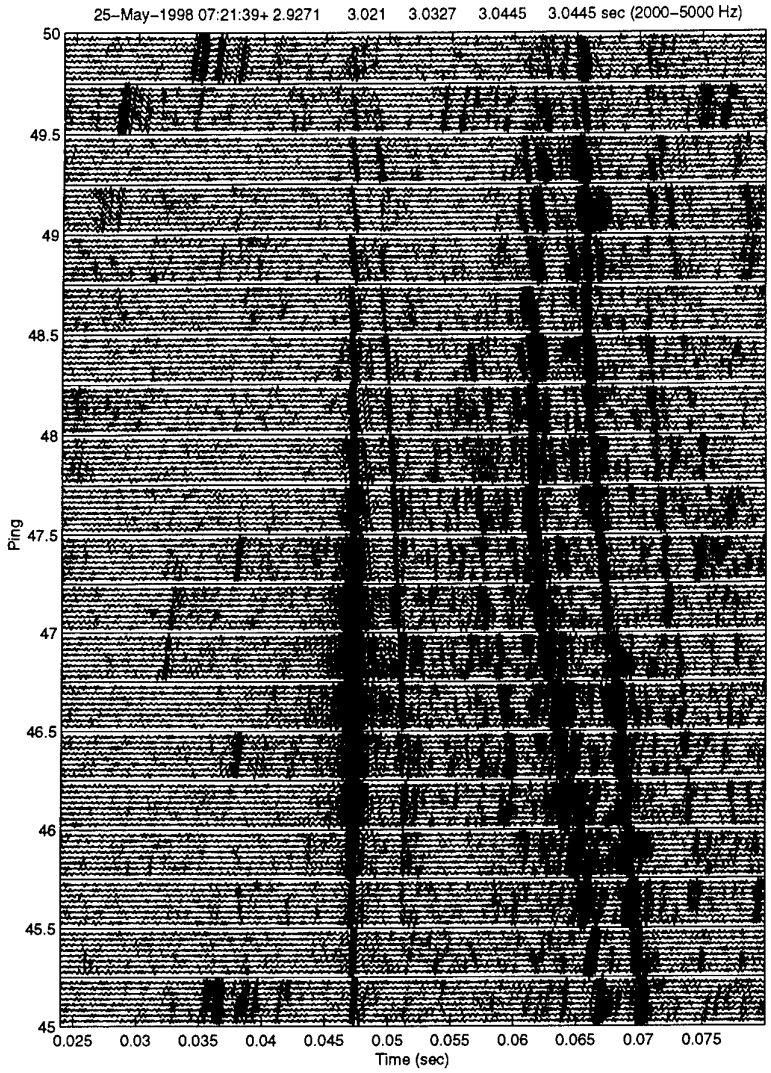

Figure 38 *Time series for files 045-049 from mission x9814501 clearly show both a large direct and surface-bounce return from the half-buried target S3, which is visible over the entire bistatic aperture between 0.062 and 0.07 s, and a slightly weaker direct return from the flush-buried target S2, visible as a precursor to the S3 return at about 0.058 s near the centre of the aperture. Note that the surface reflected portion of the S2 arrival is masked by the direct arrival from S3. The strong arrival near time 0.047 s is the direct arrival. The direct arrivals were selected from a similar display of the unsynchronized data. The standard deviation of the unsynchronized arrivals was approximately 50 ms, due to the inaccuracy of the TOPAS trigger. The detection of the S2 target is enhanced by the favorable bistatic configuration during this portion of the experiment.*

The results discussed in this section serve to illustrate that bistatic target imaging using the mobile AUV platform is feasible. In the three data segments analyzed, the partially buried sphere S3 was clearly visible in all cases. In one case, for data files 045-049, the flush buried sphere S2 is also located, due to the favorable bistatic geometry. The results in general indicate that there are significant unresolved biases in the AUV navigation. With sufficient improvements in navigation, more aggressive imaging techniques, ranging from the simple inclusion of more bandwidth, through coherent imaging and non-linear imaging techniques, could be pursued. However, even at the current level of refinement, there is sufficient evidence to suggest that there is significant potential for improved target localization through the use of one or more bistatic AUV receivers. These types of receivers are unique in that they have the flexibility to survey potential targets at favorable bistatic angles. It is this flexibility which can lead to significant performance gains over more traditional, monostatic receiver geometries.

5.8 Seismic target excitation

In the seismic excitation experiment, a shotgun source was positioned on the seabed in line with the buried hydrophone array, as shown in Fig. 39. The signals created by two shotgun firings were recorded on the buried array, the HLA in bistatic configuration, and by the AUV array during two legs of its standard survey pattern. Figure 39 shows the navigated position of the AUV at the times of the two shotgun firings. Preliminary analysis of the AUV data focused on identifying the direct blast and its multiples, and determining whether the target scattering of the various incident seismic waves, including the Scholte waves, could be identified in the time series.

This analysis was performed using a simple ray-tracing calculation, using the known target field geometry and the AUV navigation data, and applying the well-defined direct blast as a timing reference.

Figures 40 and 41 show the time series recorded on the AUV array during the two shotgun firings identified by the associated acoustic data files, x9814403-22 and x9814403-49. The arrival identification assumes that the targets are excited by compressional waves. The nominal compressional wave speeds of 1700m/s for the bottom and 1500m/s for the water column were used in the arrival estimation. In addition to the direct blast and its multiples, several target returns are identifiable, in particular those associated with the spheres S2, S3 and the cylinder C2, while little evidence exist for seismic scattering from the other targets. Only the direct and the first surface-reflected paths were considered here.

The time series x9814403-22 were collected during the first shotgun firing on an inbound leg of the AUV survey, with the shotgun source and target field being

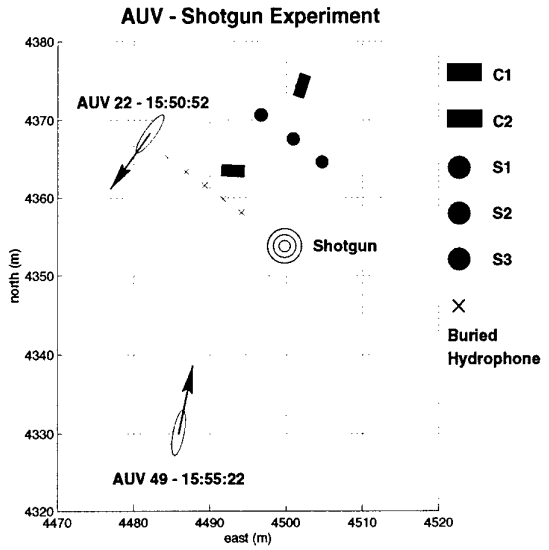

Figure 39 *Shotgun experiment scenario. A bottom mounted shotgun device was fired twice during an AUV survey mission. The two positions of the AUV are shown. The shotgun generates seismic interface (Scholte) waves, which propagate at low speed, and are scattered into acoustic waves which are received by the fixed and mobile arrays.*

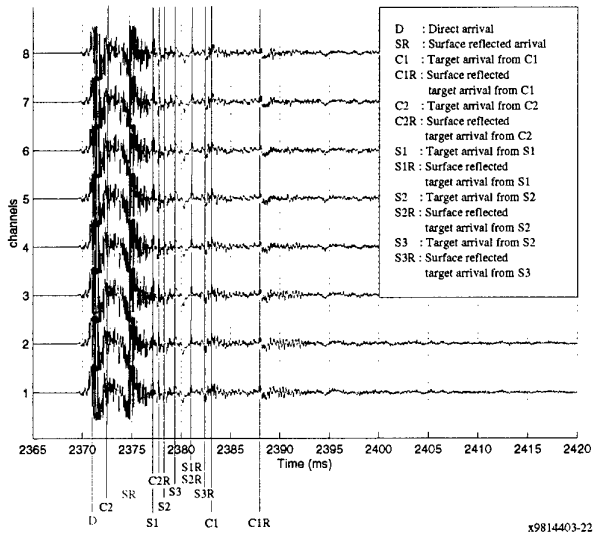

Figure 40 *Shotgun signals recorded on the AUV 'swordfish' array during firing of the seabed-mounted shotgun source with AUV in broadside, forward-scatter configuration (AUV 22).*

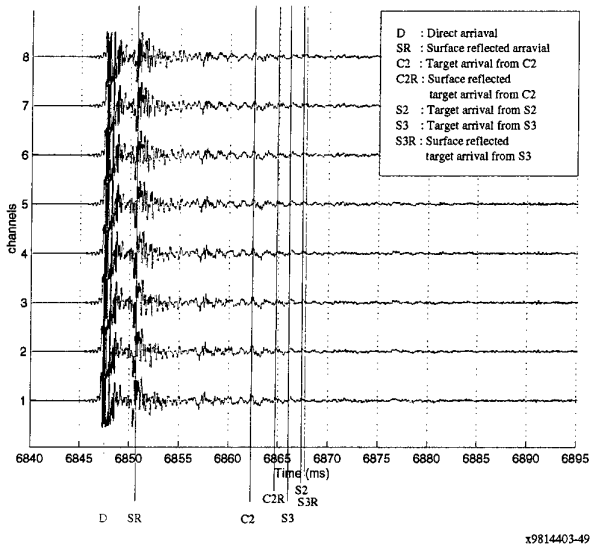

Figure 41 *Shotgun signals recorded on the AUV 'swordfish' array during firing of the seabed-mounted shotgun source with AUV in end-fire, backscatter configuration (AUV 49).*

approximately broadside to the AUV array ('AUV 22' in Fig. 39). In this forward scatter configuration, the direct and surface-reflected target signals arrive with small time separations (< 17 ms). Here the strongest target signals are the direct target signal from C2.

The time series x9814403-49, collected at position 'AUV 49' in Fig. 39, have a significantly different arrival structure because the AUV is here in a backscatter configuration. Therefore, the signals from the direct blast and its surface reflection are well separated in time from the target signals.

In contrast to the previous configuration, the scattering from S1 cannot be identified, probably because of the deep burial of this target and the sub-critical AUV configuration. Arrivals from the cylinder C1 could not be clearly identified either.

Preliminary analysis suggests that the scattering of the seismic interface waves is relatively insignificant compared to the compressional wave scattering. This is probably associated with very low excitation of these waves due to low shear speed, a hypothesis which appears consistent with the signals observed on the buried hydrophone array.

6

Conclusions and future work

The GOATS'98 experiment clearly demonstrated that AUV technology is now mature enough that small, inexpensive vehicles can be operated reliably in shallow to very shallow water, launched and recovered from a surface ship offshore. Also, it was demonstrated that AUV technology is extremely useful as an acoustic test platform for new sonar concepts for littoral MCM.

Given the new, untested systems deployed, GOATS'98 was clearly a high-risk operation, but the payoff was significant. The data set collected, relating to 3-D target scattering and reverberation, is unique in terms of spatial sampling, number and type of targets, and insonification geometry. This data set will support a multi-year analysis effort, which is planned as a collaborative effort between SACLANTCEN and MIT. The main objectives of this analysis will be to validate the numerical scattering and reverberation models and to identify robust features and patterns in the 3-D target scattering, which can be searched for, in a combined detection and classification procedure.

The next step towards the development of new multi-platform MCM sonar concepts, which is the long term objective of the GOATS effort, is to design control procedures for multiple AUV's which adaptively identify these acoustic features. GOATS'98 also provided the first step in this direction. It was demonstrated that the AUV can be used as an acoustic platform with very low self-noise characteristics. Also, it was demonstrated that AUV's can be reliably operated from offshore platforms such as R/V *Alliance*, and navigate with accuracy of few metres into shallow and very shallow water less than 100 m from shore and complete complex, accurate, pre-designed survey patterns.

The AUV technology must still undergo refinements before becoming a standard operational asset. The most important shortcoming is the expertise needed for programming the AUV missions. Here an obvious next step is to develop a graphical user interface that allows an untrained user to design a mission using a standard toolkit of behaviors, download it to the AUV and hand over the vehicle launch to a trained deck crew.

Another refinement is a robust and automatic procedure for synchronizing the vehicle clock with surface systems. Many AUV applications are not time critical on

scales less than a second, but this is a key factor for acoustic measurements. Options include GPS receivers or automatic, computer network, time-synchronization daemons.

The long-baseline acoustic navigation system, worked in a satisfactory manner in terms of providing way-point navigation of the surveys with an accuracy of a few metres. However, the analysis of the acoustic data and the altimeter detections of the HLA revealed a significant bias depending on the direction of the AUV. This navigation performance is inadequate for synthetic aperture, bistatic imaging and for most MCM sonar. In GOATS'98, the direct TOPAS signal and its multiples were used to provide micro-navigation, but an independent approach would be highly desirable for using the AUV for sampling the 3-D field in general. Alternative, high-resolution navigation approaches should therefore be considered for use within the survey area.

The launch and recovery procedures when operating from a ship like *Alliance* should also be refined. A number of successful 'quick-release' launches were performed in GOATS'98, but the recovery always required the work boat. This is particularly limiting for night operations, which are certainly possible as demonstrated recently by MIT in Labrador Sea. A radio modem on the AUV would allow communication after surfacing, and a return mission could be downloaded to bring the AUV autonomously back alongside *Alliance* for recovery from the deck.

The *Alliance* can become an extremely useful platform for UUV (ROV or AUV) operations, with its extensive laboratory facility, and the 'garage' which is close to ideal for vehicle preparation and repair. However, a few changes are needed with regard to implementation of state-of-the-art acoustic navigation capabilities, which will integrate the UUV navigation with the ship's navigation system. Some integration was achieved in GOATS'98, with the ship navigation data being imported into the AUV navigation system, but a two-way integration is highly desirable for multi-vehicle operations and for operations with *Alliance* in motion.

In terms of future effort towards the development of a new adaptive, multi-platform MCM sonar concept, the suggestions following GOATS'98 are:

- The effort should be expanded to incorporate multiple UUV's, most conveniently, a general-purpose *master* ROV tethered to *Alliance* and two or more AUV's. The ROV will eliminate the need for the shore facility, making most operations possible from *Alliance*. The multiple AUV's will allow for true multi-platform measurements, and the development of adaptive, multi-vehicle control procedures.

- Conventional sources, insonifying larger areas of the seabed should be considered in conjunction with multiple receivers, to investigate the coverage perfor-

mance of multistatic systems.

- In the longer term, low-and high frequency sonar concepts should be used in concert. One of the outcomes of a continued effort is to determine an optimal mix of such sensor systems.
- Adaptive sampling procedures for the robust acoustic signatures must be determined, and the associated AUV adaptive control issues must be resolved.
- Acoustic communication is critical to the multi-AUV concept and should be incorporated in the next iteration.
- Navigation approaches other than LBL/USBL should be explored, in particular for clandestine operation. For the continued research phase, a more accurate LBL network should be applied.
- The time-synchronization issue regarding the sources and the fixed and mobile arrays is critical and should be resolved before the next AUV acoustic experiment.

Acknowledgements

The assistance of A. Lyons and B. Zerr in processing the stereo-photography and seafloor mapping data, respectively, is highly appreciated.

The MIT component of GOATS'98 was supported by the US Office of Naval Research, in part by the Ocean Modeling and Prediction Program and the Ocean Acoustics Program.

References

[1] T. Curtin, J.G. Bellingham, J. Catipovic, and D. Webb. Autonomous oceanographic sampling networks. *Oceanography*, **6**, 1993:86–94.

[2] H. Schmidt, J.G. Bellingham, and P. Elisseef. Acoustically focused oceanographic sampling in coastal environments. *In*: Pouliquen, E., Kirwan, A.D., Jr., Pearson, R.T., editors. Rapid Environmental Assessment, SACLANTCEN CP-44. La Spezia, Italy, SACLANT Undersea Research Centre, 1997: pp. 145-151.

[3] Labrador sea expedition – 19 Jan - 18 Feb '98 - autonomous ocean sampling network experiment. MIT Sea Grant AUV Laboratory, *http://cook.mit.edu/~auvlab/LabSummary.html.*, 1998.

[4] H. Schmidt, J. Lee, H. Fan, and K. LePage. Multistatic bottom reverberation in shallow water. *In*: N.G. Pace, E. Pouliquen, O. Bergem, and A.P. Lyons, editors, High Frequency Acoustics in Shallow Water. SACLANTCEN CP-45. La Spezia, Italy, SACLANT Undersea Research Centre, 1997: pp. 475-482.

[5] E. Pouliquen, A. Lyons, and N.G. Pace. Penetration of acoustic waves into sandy seafloors at low grazing angles: The Helmholtz–Kirchhoff approach. SR-290. La Spezia, Italy, SACLANT Undersea Research Centre, 1998.

[6] A. Maguer, E. Bovio, W.L.J. Fox, E. Pouliquen, and H. Schmidt. Mechanisms for subcritical penetration into a sandy bottom: Experimental and modeling results. SACLANTCEN SR-287. La Spezia, Italy, SACLANT Undersea Research Centre, 1998.

[7] H. Schmidt. Physics of 3-D scattering from rippled seabeds and buried targets in shallow water. SACLANTCEN SR-289. La Spezia, Italy, SACLANT Undersea Research Centre, 1998.

[8] J. Fawcett. Finite element modelling of three-dimensional scattering from azimuthally-symmetric elastic shells. SACLANTCEN SR-273. La Spezia, Italy, SACLANT Undersea Research Centre, 1998.

[9] W.L.J. Fox and A. Maguer. Detection of buried objects at low grazing angles: Preliminary experimental results. SACLANTCEN SR-293. La Spezia, Italy, SACLANT Undersea Research Centre, 1998.

[10] Bentech Subsea AS, Stjørdal, Norway. *Simrad TOPAS PS 040 Operator Manual.*

[11] O. Bergem and N.G. Pace. Calibration of the TOPAS PS040. Part I: Measurements recorded with TOPAS acquisition system. SACLANTCEN SM-119. La Spezia, Italy, SACLANT Undersea Research Centre, 1996.

[12] S. Fioravanti, A. Maguer, W.L.J. Fox, L. Gualdesi, and A. Tesei. Underwater rail facility for highly controlled experiments at sea. Submitted to Third European MAST Conference, Lisbon, Portugal, 1998.

[13] A. P. Lyons, T. Akal, and E. Pouliquen. Measurement of seafloor roughness with close range digital photogrammetry. To appear in Proceeding of Oceans '98, Sep. 1998.

Document Data Sheet

NATO UNCLASSIFIED

Security Classification		Project No.
UNCLASSIFIED		033-4
Document Serial No.	**Date of Issue**	**Total Pages**
SR-302	October 1998	68 pp.

Author(s)

Schmidt, H., Maguer, A., Bovio, E., Fox, W.L.J., LePage, K., Pace, N.G., Hollett, R., Guerrini, P., Sletner, P.A., Michelozzi, E., Moran, B., Grieve, R.

Title

Generic Oceanographic Array Technologies (GOATS)`98 -- Bi-static Seabed Scattering Measurements using Autonomous Underwater Vehicles

Abstract

The GOATS`98 experiment was performed May 5-29, 1998 in shallow water off Marciana Marina, on the island of Elba. The experiment addressed some of the fundamental issues associated with using the new Autonomous Ocean Sampling Network (AOSN) concept for mine countermeasures and rapid environmental assessment in very shallow water. A parametric source, mounted on a tower was used to insonify proud and buried seabed targets. Target scattering and reverberation was measured by several fixed arrays and a mobile array mounted on an autonomous underwater vehicle. This extensive receiving array capability was used to map the full 3-D structure of scattering and reverberation, the objective being to identify 3-D acoustic features, which distinguish targets from the reverberant background and which may therefore be applied for combined detection and classification. The use of the AUV at the same time, addressed various issues associated with the use of the AOSN concept for measuring such features by providing mobile platforms for both mono-, bi- and multi-static sonar configurations. The experiment demonstrated clearly that AUV technology is now sufficiently mature, to enable small, inexpensive vehicles to be operated reliably in very shallow water, launched and recovered from a surface ship off-shore. The excellent quality of the 3-D acoustic data sets, recorded during the experiment, demonstrated that AOSN technology can become extremely useful as an acoustic platform for new sonar concepts, for littoral MCM.

Keywords

mine countermeasures - sonars - reverberation - target scattering - shallow water - underwater vehicles

Issuing Organization

North Atlantic Treaty Organization
SACLANT Undersea Research Centre
Viale San Bartolomeo 400, 19138 La Spezia, Italy
[From N. America: SACLANTCEN (New York) APO AE 09613]

Tel: +39 0187 527 361
Fax:+39 0187 524 600 E-mail:
library@saclantc.nato.int

NATO UNCLASSIFIED

Initial Distribution for SR-302

Ministries of Defence

DND Canada	10
CHOD Denmark	8
MOD Germany	15
HNDGS Greece	12
MARISTAT Italy	9
MOD (Navy) Netherlands	12
NDRE Norway	10
MOD Portugal	5
MDN Spain	2
TDKK and DNHO Turkey	5
MOD UK	20
ONR USA	32

NATO Commands and Agencies

NAMILCOM	2
SACLANT	3
CINCEASTLANT/ COMNAVNORTHWEST	1
CINCIBERLANT	1
CINCWESTLANT	1
COMASWSTRIKFOR	1
COMSTRIKFLTANT	1
COMSUBACLANT	1
SACLANTREPEUR	1
SACEUR	2
CINCNORTHWEST	1
CINCSOUTH	1
COMEDCENT	1
COMMARAIRMED	1
COMNAVSOUTH	1
COMSTRIKFORSOUTH	1
COMSUBMED	1
NC3A	1
PAT	1

Scientific Committee of National Representatives

SCNR Belgium	1
SCNR Canada	1
SCNR Denmark	1
SCNR Germany	1
SCNR Greece	1
SCNR Italy	1
SCNR Netherlands	2
SCNR Norway	1
SCNR Portugal	1
SCNR Spain	1
SCNR Turkey	1
SCNR UK	1
SCNR USA	2
SECGEN Rep. SCNR	1
NAMILCOM Rep. SCNR	1

National Liaison Officers

NLO Canada	1
NLO Denmark	1
NLO Germany	1
NLO Italy	1
NLO Netherlands	1
NLO Spain	1
NLO UK	1
NLO USA	1

Sub-total	188
SACLANTCEN	30
Total	218